Na *et al. Biochar* (2026) 8:118
https://doi.org/10.1007/s42773-026-00630-y

Biochar

ORIGINAL RESEARCH

Open Access

# Microbial life-history strategies mediate differential effects of straw and biochar amendments on soil POC/MAOC dynamics and SOC sequestration

Liping Na[1], Yalin Liu[2], Qiong Nan[3], Litian Chen[1,4], Da Dong[4], Weixiang Wu[3], Jiangwu Tang[1], Shengmao Yang[1,5] and Yuxue Liu[1,4,5,6*]

## Abstract

Enhancing soil organic carbon (SOC) sequestration in paddy soils is a critical strategy for climate change mitigation. However, the mechanistic underpinnings of how substrate quality modulates microbial life-history strategies to regulate the formation and stabilization of distinct SOC fractions—particulate organic carbon (POC) and mineral-associated organic carbon (MAOC)—remain poorly understood. We conducted a 65-day incubation experiment using $^{13}$C-labeled rice straw and straw-derived biochar to disentangle the relationships among energy inputs, microbial strategies, and SOC stabilization pathways. Both straw and biochar amendments increased SOC content, with biochar inducing a 103% increase compared to only 38.7% from straw. Straw improved nutrient availability (e.g., dissolved organic carbon and microbial biomass carbon) and stimulated the activities of β-glucosidase, β-1,4-N-acetylglucosaminidase, leucine aminopeptidase, and acid phosphatase, thereby enriching r-strategist microbes (e.g., Mortierellomycota and Firmicutes). This promoted fungal-mediated POC formation and MAOC accumulation derived from bacterial necromass. However, straw induced a positive priming effect, accelerating the mineralization of native SOC and resulting in a carbon sequestration efficiency of only 22.8% by day 65. In contrast, biochar alleviated microbial nitrogen demand, redirected microbial activity toward the decomposition of recalcitrant carbon, and enriched *K*-strategist microbes (Actinobacteriota and Chloroflexi). These shifts further facilitated MAOC accumulation via bacterial necromass formation, while inducing a negative priming effect that minimized native carbon loss, achieving a carbon sequestration efficiency of 99.7% at the end of the incubation. Our findings reveal that straw and biochar enhance SOC sequestration through distinct microbial pathways: straw drives rapid but less efficient carbon accumulation via r-strategist microbial activity, whereas biochar promotes stable and highly efficient sequestration through *K*-strategist-mediated processes. These results highlight the importance of substrate quality in shaping microbial community dynamics and SOC sequestration outcomes, providing a mechanistic basis for optimizing organic amendment strategies in paddy agroecosystems.

## Highlights

- Biochar boosts SOC via negative priming and *K*-strategies, outcompeting straw.
- Straw elevates POC and MAOC but priming limits overall sequestration.

*Correspondence:
Yuxue Liu
liuyuxue505@163.com
Full list of author information is available at the end of the article



Springer

- Straw favors r-strategists: Mortierellomycota boosts POC, Firmicutes promotes MAOC via necromass.
- Biochar enriches *K*-strategists (Actinobacteriota, Chloroflexi), boosting MAOC.

**Keywords** Soil organic matter, Particulate organic matter, Mineral-associated organic matter, r-strategists, *K*-strategists, Biochar amendment

**Graphical Abstract**

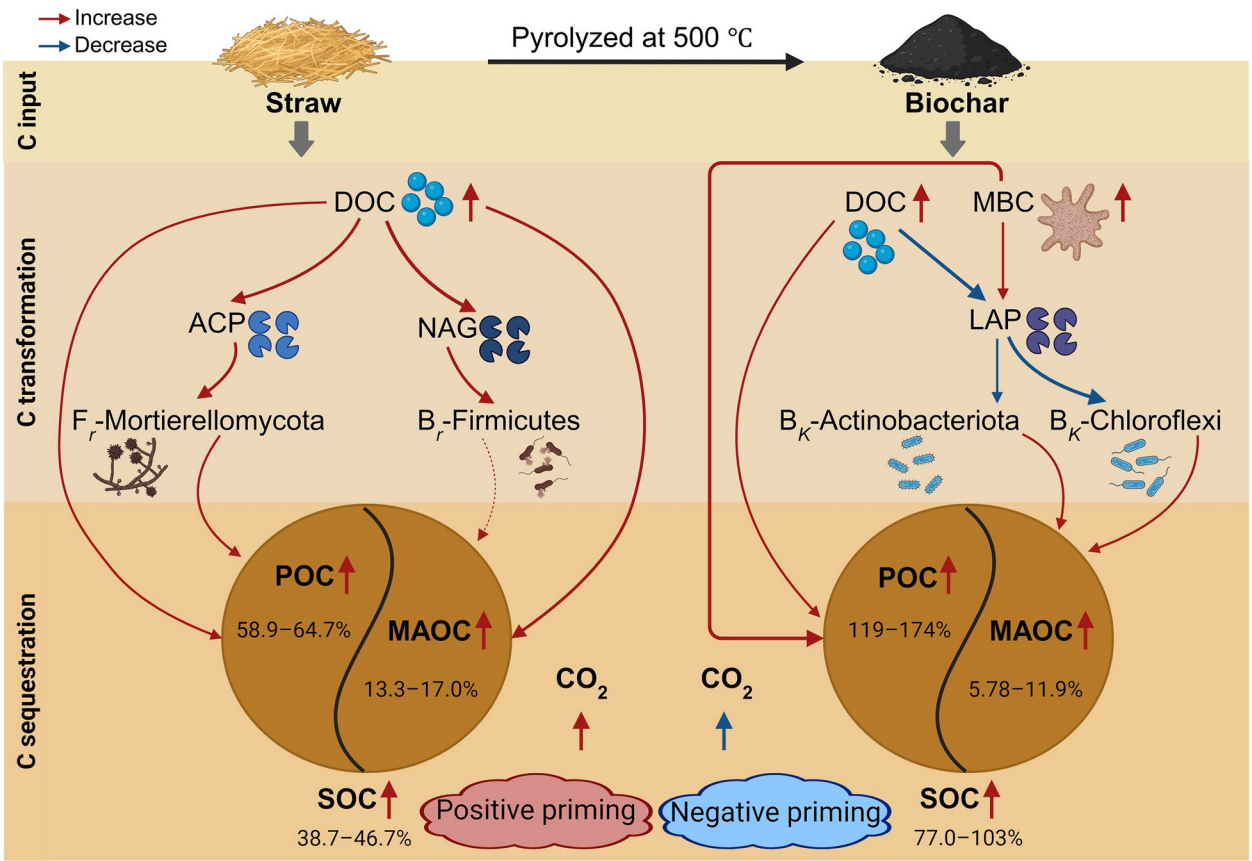


## 1 Introduction

Soil, the largest terrestrial carbon (C) pool, stores approximately 2400 Gt of C within the 0–2-m depth globally (Beillouin et al. 2023). Enhancing soil organic carbon (SOC) sequestration is a crucial strategy for mitigating global warming. An annual increase of 4‰ in SOC stock (equivalent to ~ 2.5 Gt C year$^{-1}$) could offset approximately 30% of global greenhouse gas emissions (Minasny et al. 2017). SOC accumulation depends on the trade-off between two functional fractions, namely particulate organic carbon (POC) and mineral-associated organic carbon (MAOC), which represent a relatively labile C pool and a stabilized C pool in the soil, respectively (Tivet et al. 2013). POC is primarily derived from partially decomposed plant residues and undergoes rapid turnover, while MAOC is largely formed from microbial metabolites and cellular residues interacting with soil mineral components, serving as the core reservoir that determines the long-term soil C sequestration capacity (Lavallee et al. 2020).

The input of exogenous C (e.g., straw and biochar) with differential energy availability drives distinct microbial metabolic pathways, thereby affecting the dynamics of POC and MAOC and thus SOC sequestration. Previous studies have demonstrated that straw increases POC and MAOC by 33% and 9.6%, respectively, whereas long-term

biochar amendment (13 years) elevates POC by fivefold and MAOC by 1.2-fold compared to no amendment (Lei et al. 2024; Zhou et al. 2025b). However, while the differential effects of these amendments on C storage are well-documented, the underlying microbial mechanisms, particularly how substrate quality filters microbial traits to regulate specific C fractions, remain to be fully elucidated.

The distinct energy properties of straw and biochar fundamentally shape the soil microbial landscape. Straw amendment provides a rich source of high energy and readily available C for soil microorganisms, stimulating the metabolism of fast-growing r-strategist microbes (Shang et al. 2023; Xu et al. 2024). These organisms drive rapid decomposition and stabilization of the SOC pool (Chen et al. 2023; Liang et al. 2017), dominating the initial phase of straw transformation (Liebich et al. 2006). Studies have shown that full straw return (100%) increased the abundance of r-strategist bacteria by 163.4% compared with the control (Wang et al. 2026). In contrast, straw-derived biochar represents a low-energy, recalcitrant C source with a highly aromatic and recalcitrant structure, coupled with a high specific surface area and strong adsorption capacity (Lehmann et al. 2006; Leng et al. 2021). These properties facilitate modifications to the soil microenvironment, promoting colonization by oligotrophic, slow-growing *K*-strategist microbes (Shang et al. 2023). Research indicates that the increase in topsoil SOC is due to a shift in the microbial community toward *K*-strategists, which in turn produce more recalcitrant necromass compounds, thereby elevating the microbial necromass C content (Luo et al. 2023; Yang et al. 2026).

The principle that microbial life-history strategies dictate SOC fractions is further supported by studies examining other environmental perturbations. For instance, warming-induced shifts in bacterial communities from *K*- to r-strategists have been shown to increase POC but decrease MAOC in black soils, as r-strategists facilitate the rapid mineralization of organic compounds while *K*-strategists are associated with more stable C pools (Lyu et al. 2025). Similarly, vegetation type can act as a filter: leguminous cover crops promote *K*-strategists (e.g., *Ilumatobacter* and *Bradyrhizobium*), enhancing SOC stability and recalcitrance, whereas non-leguminous cover crops enrich r-strategists (e.g., *Lysinibacillus* and *Paenibacillus*), corresponding to greater labile C accumulation (Liu et al. 2025b). Furthermore, increased precipitation has been found to shift bacterial communities toward r-strategy in both rhizosphere and bulk soils, with the enrichment of r-strategists promoting rhizosphere MAOC accumulation by enhancing root C exudation (Zeng et al. 2025). Despite these insights, a mechanistic understanding of how substrate energy quality acts as a filter for these microbial life-history strategies to regulate the trade-off between POC and MAOC formation is lacking. Specifically, it remains unclear whether POC and MAOC accumulation in paddy soils is driven primarily by the high-turnover necromass pump associated with r-strategists or by the high-efficiency metabolic traits of *K*-strategists.

In this study, an incubation experiment was conducted to address the following scientific questions: (1) What are the dynamic effects of straw and biochar amendments on SOC fractions (POC and MAOC)? (2) How do straw and biochar amendments influence POC and MAOC by regulating microbial life-history strategies? We hypothesized that straw amendment enhances the accumulation of both POC and MAOC by enriching r-strategist microorganisms, whereas biochar amendment promotes MAOC accumulation by enriching *K*-strategists through the formation of microbial necromass. This study provides a theoretical basis for revealing the C sequestration mechanisms of soil microorganisms under different exogenous C inputs, and provides practical guidance for optimizing agricultural management measures to enhance SOC sequestration.

## 2 Materials and methods

### 2.1 Preparation of soil, straw, and biochar

Paddy soil samples were collected from the 0–20 cm topsoil layer at the Yangdu Research Station of the Zhejiang Academy of Agricultural Sciences, located in Jiaxing City, Zhejiang Province (120° 24′ 23″ E, 30° 26′ 07″ N). The experimental field has been under a rice-rape rotation system since 2011. A five-point sampling method was employed across a 10 m × 10 m plot, with approximately 2 kg of soil collected from each point. All collected soil was thoroughly homogenized to form a single composite sample. Visible plant roots and large organic residues were manually removed from the composite sample. The soil was then air-dried and passed through a 2-mm sieve; the sieved soil was split into two portions, one for analysis of basic physicochemical properties and the other for use in the subsequent incubation experiment.

The $^{13}C$-labeled rice straw and rice straw-derived biochar were used as exogenous C sources and prepared as follows. The $^{13}C$-labeled straw was obtained by an isotope pulse labeling method (Lu et al. 2004). Briefly, stable isotope $^{13}C$ labeling was conducted for 6 days in a closed plexiglass chamber between 9:00 and 15:00 on sunny days. At the beginning of labeling, $Ba^{13}CO_3$ (> 98%) powder was pre-placed in a beaker, which was then placed inside the sealed chamber together with the rice plants. A detector and a thermometer were used to monitor the $CO_2$ concentration and the temperature in the chamber,

respectively. When the $CO_2$ concentration dropped from 350 to 125 ppm, an appropriate amount of 1 mol $L^{-1}$ hydrochloric acid was added through a hose to react with the $Ba^{13}CO_3$, maintaining the indoor $CO_2$ concentration within the range of 250–300 ppm. After labeling, the straw was collected and subjected to inactivation at 105 ℃ for 30 min followed by drying at 60 ℃ for 12 h. To obtain $^{13}C$-labeled biochar, a portion of the $^{13}C$-labeled straw was pyrolyzed at a heating rate of 5 ℃ $min^{-1}$ to a maximum temperature of 500 °C and held for 2 h before cooling to room temperature. Finally, straw and biochar were crushed and ground to a particle size of less than 2 mm for subsequent use.

The basic physicochemical properties of the soil, straw, and biochar samples were determined using the following methods. Soil available phosphorus was determined by the $NH_4F$-HCl extraction followed by the molybdenum-antimony colorimetric method (Bray and Kurtz 1945). Soil available potassium was measured using ammonium acetate extraction coupled with flame photometry (Helmke and Sparks 1996). Straw and biochar samples were subjected to digestion with a $HClO_4$–HF solution. Total potassium in the digests was determined by flame spectrophotometry, while total phosphorus was analyzed using the phosphomolybdate colorimetric method (Bao 2000; Murphy and Riley 1962). Ash content was determined by combusting samples at 750 ℃ for 6 h, while volatile matter content was quantified based on weight loss after heating samples at 900 ℃ for 7 min in a tightly covered crucible (Zhao et al. 2017). The surface area and porosity of straw and biochar were characterized using a NOVA 2200e analyzer (Quantachrome Instruments, Boynton Beach, FL, USA) at the temperature of liquid nitrogen (77 K). The specific surface area was calculated using the Brunauer–Emmett–Teller (BET) method, and the average pore size was derived from the adsorption–desorption isotherms (Zhao et al. 2017). The $\delta^{13}C$ values and physicochemical properties of the soil, straw and biochar are presented in Table 1.

### 2.2 Incubation experiment

Three treatments were included in the incubation experiment: (1) no straw or biochar amendment (CK), (2) $^{13}C$-labeled rice straw (ST) amendment, and (3) $^{13}C$-labeled rice straw-derived biochar (BC) amendment. The experiment was designed with six replicates per treatment. Three replicates were destructively sampled on the 10th day, while the remaining three were used for gas collection throughout the incubation period and destructively sampled on the 65th day.

To activate and stabilize indigenous microorganisms, all soils were pre-incubated for 7 days at 40% of the field water-holding capacity prior to the formal experiment. Then, 100 g air-dried soil was thoroughly mixed with 4 g C $kg^{-1}$ of straw or biochar (a moderately increased application rate selected to ensure that the treatment effects could be appropriately detected), and soil moisture was adjusted to 60% of water-holding capacity (Kalu et al. 2024) using deionized water for the formal incubation experiment. All incubations were carried out in a dark environment at a constant temperature of 25 ± 1 ℃ for 65 days.

### 2.3 Sampling and analysis

A total of 21 gas samples were collected during the incubation period. The content and $\delta^{13}C$ abundance of $CO_2$ were determined by an isotope ratio mass spectrometer (MAT 253) equipped with a gas chromatograph (Agilent 7820, Agilent Technologies, Santa Clara, CA, USA). Briefly, incubation flasks were evacuated prior to gas collection, then filled with simulated air ($CO_2$-free air) and sealed. After 24 h, 30 mL of gas sample was collected using a 50 mL sealed syringe (Shanghai Boli Pigeon Industry and Trade Co., Ltd.). Before each sampling, the syringe plunger was pulled and pushed three times to homogenize the gas mixture (Wang et al. 2025c). The collected gas samples were stored in sealed gas sampling cylinders (Nichiden-Rika Glass Co., Ltd.).

Destructive soil samplings were performed on the 10th and last days of incubation to determine SOC, POC, MAOC, pH, dissolved organic carbon (DOC), microbial biomass carbon (MBC), total nitrogen (TN), microbial biomass nitrogen (MBN), ammonium nitrogen ($NH_4^+$–N), nitrate nitrogen ($NO_3^-$–N), enzyme activities and the microbial community compositions of fungi and bacteria. SOC and TN were determined

**Table 1** Basic characteristics of soil, straw, and biochar used in this experiment

| | C (%) | $\delta^{13}C$ (‰) | N (%) | P (%) | K (%) | C:N ratio | pH | Ash (%) | Volatile matter (%) | Surface area ($m^2$ $g^{-1}$) | Average pore size (nm) |
|---|---|---|---|---|---|---|---|---|---|---|---|
| Soil | 0.89 | −24.38 | 0.10 | 0.01[a] | 0.10[a] | 8.99 | 6.48 | / | / | / | / |
| Straw | 37.12 | 2015.42 | 0.93 | 0.32 | 1.00 | 39.79 | 6.01 | 10.30 | 38.64 | 2.52 | 10.01 |
| Biochar | 54.22 | 2498.37 | 1.60 | 0.84 | 3.88 | 33.94 | 10.05 | 29.81 | 19.80 | 5.76 | 14.31 |

[a] Available content

using an elemental analyzer (Vario MACRO Cube, Germany). Soil pH was measured in a soil-to-water suspension (1:2.5, w/v) with a pH meter (PHS-3C, China). DOC was extracted from soil samples using deionized water at a soil-to-water ratio of 1:5 (w/v). The filtrate was passed through a 0.45 μm membrane filter, and DOC concentration was quantified using a TOC analyzer (Vario TOC select, Elementar, Germany) (Ghani et al. 2003). MBC and MBN were determined via the chloroform fumigation-direct extraction method, with 0.5 M $K_2SO_4$ as the extractant (Brookes et al. 1985). Both DOC and dissolved nitrogen (DN) concentrations in fumigated and non-fumigated extracts were analyzed using the same Vario TOC select analyzer. MBC was calculated using a conversion factor of 0.45 (Vance et al. 1987), while MBN was derived with a conversion factor of 0.54 (Brookes et al. 1985). Fresh soil samples (5 g) were extracted with 2 M KCl (1:5 soil-to-solution ratio) and filtered for $NH_4^+$–N and $NO_3^-$–N analysis according to Mulvaney (1996).

For the determination of soil POC and MAOC, soil samples were extracted using the sodium hexametaphosphate extraction method (Cambardella and Elliott 1992). In brief, 30 g soil sample was shaken with 150 mL sodium hexametaphosphate solution (5 g $L^{-1}$) in a 250 mL plastic bottle for 18 h at 100 rpm. The soil suspension was sieved through a 53 μm sieve. The fraction retained on the sieve (> 53 μm) was considered POC, while the fraction passing through the sieve (< 53 μm) was considered MAOC. All fractions were oven-dried at 60 ℃, weighed, and ground to pass through a 100-mesh sieve. One portion was analyzed for C content with a Total Organic Carbon Analyzer (Elementar, Germany), while the other was used to determine $\delta^{13}C$ values by Elemental Analyzer-Isotope Ratio Mass Spectrometry (EA-IRMS, Germany).

The activities of β-glucosidase (BG), β-1,4-N-acetylglucosaminidase (NAG), leucine aminopeptidase (LAP), and acid phosphatase (ACP) were determined using a microplate assay (Zhang et al. 2024b). The brief procedure was as follows: For the determination of BG, NAG, and ACP activities, 0.05 g of fresh soil was mixed with substrate-specific buffer solutions, followed by incubation at 37 ℃ for 1 h. After terminating the reaction with the specified stop solution, the mixture was centrifuged at 12,000 rpm for 10 min, and the absorbance of the supernatant was measured at 405 nm. For LAP activity analysis, 0.05 g of fresh soil was mixed with the corresponding substrate solution and incubated at 37 ℃ for 1 h. The reaction was terminated, and the mixture was centrifuged at 8000 rpm for 5 min. The absorbance of the supernatant was then measured at 405 nm. All enzyme activities were quantified using standard curves generated with p-nitrophenol (for BG, NAG, and ACP) or p-nitroaniline (for LAP). Activity values were normalized to dry soil weight and expressed as nmol $h^{-1}$ $g^{-1}$ dry soil.

### 2.4 Soil amino sugar analysis

Soil amino sugars were extracted and quantified following modified protocals adapted from Zhang and Amelung (1996) and Salas et al. (2023). Briefly, 0.5 g of air-dried soil subsamples were hydrolyzed with 10 mL of 6 M HCl at 105 ℃ for 6 h. The resulting hydrolysates were filtered through 0.45 μm cellulose acetate membrane filters (Sartorius, Goettingen, Germany) and collected into 20 mL scintillation vials. After evaporation to dryness using a nitrogen stream, the residues were redissolved in 12 mL of Milli-Q water.

The solutions were then transferred to 50 mL Falcon tubes, and the pH was adjusted to 6.6–6.8 using 1 M KOH. To remove iron-containing precipitates, samples were centrifuged at 1,600 × g for 15 min, and the resulting supernatants were freeze-dried. The dried residues were redissolved in 8 mL of methanol, followed by centrifugation at 1,600 × g for 10 min to eliminate insoluble debris. The clarified methanol supernatants were transferred into 10 mL cryovials (Simport, polypropylene T310-10A) and evaporated to dryness under nitrogen. The final residues were reconstituted in 1 mL of Milli-Q water.

Amino sugars were derivatized with 1-methyl-3-phenyl-2-pyralozone (PMP) prior to LC–MS analysis, following the method described by Salas et al. (2023). Specifically, samples were mixed with 0.5 M PMP solution and the derivatization reaction was conducted in a water bath at 70 ℃. Following the reaction, formic acid was added to neutralize the reaction mixture. Excess PMP was removed via liquid–liquid extraction with chloroform and the upper aqueous layer was retained. The aqueous phase was filtered through a 0.2 μm acetate membrane syringe filter (VWR International™) before instrumental analysis.

Analyses were performed using a UPLC Ultimate 3000 system coupled to an Orbitrap Q Exactive HRMS system. Chromatographic separation was achieved on a Waters AccQ.Tag Ultra C18 column, and the mass spectrometer was operated in ESI + mode, with a full-scan range of 150–1000 m/z. Finally, four microbial necromass biomarkers were quantified: muramic acid (MurA), mannosamine (ManN), galactosamine (GalN), and glucosamine (GlcN).

### 2.5 High-throughput sequencing

Soil DNA was extracted from the samples using the E.Z.N.A.® soil DNA Kit (Omega Bio-tek, Norcross, GA, U.S.). The purity and concentration of DNA were quantified using a NanoDrop2000 spectrophotometer (Thermo Scientific, United States). For the bacterial

community, the bacterial 16S rRNA genes were amplified using the universal bacterial primers 27F (5'-AGRGTT YGATYMTGGCTCAG-3') and 1492R (5'-RGYTACCTT GTTACGACTT-3')(Weisburg et al. 1991). For the fungal community, the ITS sequences were amplified using the primers ITS1F (5'-CTTGGTCATTTAGAGGAAGTAA-3') and ITS4R (5'-TCCTCCGCTTATTGATATGC-3') (Souza et al. 2014). Primers were tailed with PacBio barcode sequences to distinguish each sample. Amplification reactions (20-μL volume) consisted of 5×FastPfu buffer 4 μL, 2.5 mM dNTPs 2 μL, forward primer (5 μM) 0.8 μL, reverse primer (5 μM) 0.8 μL, FastPfu DNA Polymerase 0.4 μL, template DNA 10 ng and DNase-free water. The PCR amplification was performed as follows: initial denaturation at 95 ℃ for 3 min, followed by 27 cycles of denaturing at 95 ℃ for 30 s, annealing at 60 ℃ for 30 s and extension at 72 ℃ for 45 s, and single extension at 72 ℃ for 10 min, and end at 4 ℃ (T100 Thermal Cycler PCR thermocycler, BIO-RAD, USA). After electrophoresis, the PCR products were purified using the AMPure® PB beads (Pacifc Biosciences, CA, USA) and quantified with Qubit 4.0 (Thermo Fisher Scientific, USA).

Purified products were pooled in equimolar ratios, and a DNA library was constructed using the SMRTbell prep kit 3.0 (Pacifc Biosciences, CA, USA) according to PacBio's instructions. Purified SMRTbell libraries were sequenced on the PacBio Sequel IIe System (Pacifc Biosciences, CA, USA) by Majorbio Bio-Pharm Technology Co. Ltd. (Shanghai, China). High-fidelity (HiFi) reads were obtained from the subreads, generated using circular consensus sequencing via SMRT Link v11.0.

### 2.6 Classification of life-history strategies

Bacterial and fungal life-history strategies were categorized at the phylum level following established frameworks that distinguish copiotrophic (r-strategist) and oligotrophic (*K*-strategist) microorganisms (Fierer et al. 2007; Francioli et al. 2016; Nemergut et al. 2010; Phung et al. 2004; Wu et al. 2021; Yao et al. 2017). We acknowledge that life-history strategies can exhibit intraspecific variation within individual phyla; for example, the phylum Ascomycota encompasses both ruderal and stress-tolerant taxa. The classifications applied in this study reflect the dominant life-history strategies reported for these phyla under the specific environmental conditions of our experiment, and may not be universally applicable across all ecological contexts.

### 2.7 Calculation

The proportion of $CO_2$ produced by $^{13}C$-labeled rice straw/straw-derived biochar was calculated using the following equation (Li et al. 2018):

$$f_{\text{straw/biochar}} = \frac{(\delta^{13}CO_2‰_{\text{straw/biochar}} - \delta^{13}CO_2‰_{\text{control}})}{(\delta^{13}C‰_{\text{straw/biochar}} - \delta^{13}C‰_{\text{soil}})} \quad (1)$$

where $\delta^{13}CO_2‰_{\text{straw/biochar}}$ is the $\delta^{13}C‰$ value of $CO_2$ produced in the soil amended with $^{13}C$-labeled rice straw/straw-derived biochar. The $\delta^{13}CO_2‰_{\text{control}}$ is the average $\delta^{13}C‰$ value of $CO_2$ produced in the soil without $^{13}C$-labeled rice straw. The $\delta^{13}C‰_{\text{straw/biochar}}$ and $\delta^{13}C‰_{\text{soil}}$ are the $\delta^{13}C‰$ value of $^{13}C$-labeled rice straw/straw-derived biochar, and the original soil, respectively.

The production of $CO_2$ derived from straw/biochar ($CO_{2\text{straw/biochar}}$) and native SOC ($CO_{2\text{SOC}}$) was calculated as follows:

$$CO_{2\text{straw/biochar}} = CO_{2\text{total}} \times f_{\text{straw/biochar}} \quad (2)$$

$$CO_{2\text{SOC}} = CO_{2\text{total}} \times (1 - f_{\text{straw/biochar}}) \quad (3)$$

where $CO_{2\text{total}}$ represents the total $CO_2$ produced from the soil amended with $^{13}C$-labeled rice straw/straw-derived biochar.

The cumulative priming effect (PE, mg C $kg^{-1}$ soil), a strong short-term change in the turnover of SOC induced by straw/biochar addition, was calculated as:

$$\text{Cumulative PE} = CO_{2\text{SOC}} - CO_{2\text{control}} \quad (4)$$

where $CO_{2\text{control}}$ is the average value of $CO_2$ produced in the soil without $^{13}C$-labeled rice straw/straw-derived biochar.

The relative PE (%) was calculated as:

$$\text{Relative PE} = (\text{Cumulative PE}/CO_{2\text{control}}) \times 100\% \quad (5)$$

The proportion of straw/biochar-derived C in POC or MAOC was calculated as follows (Jiang et al. 2021):

$$f_C = \frac{(\delta^{13}C‰_C - \delta^{13}C‰_{\text{control}})}{(\delta^{13}C‰_{\text{straw/biochar}} - \delta^{13}C‰_{\text{control}})} \quad (6)$$

where $\delta^{13}C‰_C$ is the $\delta^{13}C‰$ value of POC or MAOC in the soil amended with $^{13}C$-labeled rice straw/straw-derived biochar. The $\delta^{13}C‰_{\text{control}}$ is the average $\delta^{13}C‰$ value of POC or MAOC in the soil without $^{13}C$-labeled rice straw/straw-derived biochar.

The "new" straw/biochar-derived C and "old" soil-derived C in POC or MAOC were calculated as follows:

$$\text{POC(MAOC)}_{\text{new}} = \text{POC(MAOC)} \times f_C \quad (7)$$

$$\text{POC(MAOC)}_{\text{old}} = \text{POC(MAOC)} - \text{POC(MAOC)}_{\text{new}} \quad (8)$$

where POC(MAOC) is the total content of POC or MAOC. $\text{POC(MAOC)}_{\text{new}}$ refers to the straw/

biochar-derived C in POC or MAOC, and $POC(MAOC)_{old}$ refers to the soil-derived C in POC or MAOC.

The net C balance (NCB) was calculated using a modified method from Wang et al. (2025b):

$$NCB = C_{straw/biochar-added} - CO_{2straw/biochar} - PE \quad (9)$$

The C sequestration efficiency was calculated using a modified method from Duan et al. (2025):

$$C\ sequestration\ efficiency = NCB/C_{straw/biochar-added} \quad (10)$$

We quantified the microbial necromass biomarker—MurA, ManN, GalN, and GlcN, and calculated bacterial necromass carbon (BNC), fungal necromass carbon (FNC), and microbial necromass carbon (MNC) using the following formulas (Meng et al. 2025):

$$BNC = MurA \times 27.67 \quad (11)$$

$$FNC = (GlcN - 1.36 \times MurA) \times 7.67 \quad (12)$$

$$MNC = BNC + FNC \quad (13)$$

### 2.8 Statistical analysis

Statistical analyses were performed using IBM SPSS Statistics (Version 26.0): one-way ANOVA was used to compare the significance of differences in various parameters among treatments ($p < 0.05$), and two-way ANOVA was employed to examine the effects of treatment, sampling time, and their interactions on the parameters. Graphs were generated using Origin 2024. Principal component analysis (PCA) was performed on the centered and standardized ASV abundance data to visualize differences in microbial community composition among treatment groups. PERMANOVA based on the Bray–Curtis dissimilarity matrix (999 permutations) was conducted to test the significance of community composition differences, with $R^2$ and $p$-values as statistical indicators. Mantel tests were used to determine the relationships between soil environmental factors, enzyme activities, life-history strategies, and SOC fractions (POC, MAOC, and SOC). The random forest model was employed to evaluate the effects of soil environmental factors, enzyme activities, and life-history strategies on SOC fractions. The influencing factors were ranked by their percentage increase in mean squared error (% IncMSE). Mantel tests (the *LinkET* package) and random forest analysis (the *randomforest* package) were performed in R 4.5.1. Key drivers of POC, MAOC, and SOC were identified through mantel tests and random forest models, and structural equation modeling (SEM) was subsequently performed in SmartPLS 4 following collinearity testing.

## 3 Results

### 3.1 Effects of straw and biochar on SOC fractions and priming effect

Compared to the control (CK) treatment, both straw and biochar amendment increased the contents of POC, MAOC, and SOC. Specifically, on day 10, straw amendment elevated POC, MAOC, and SOC by 64.7%, 17.0%, and 46.7%, respectively, whereas biochar

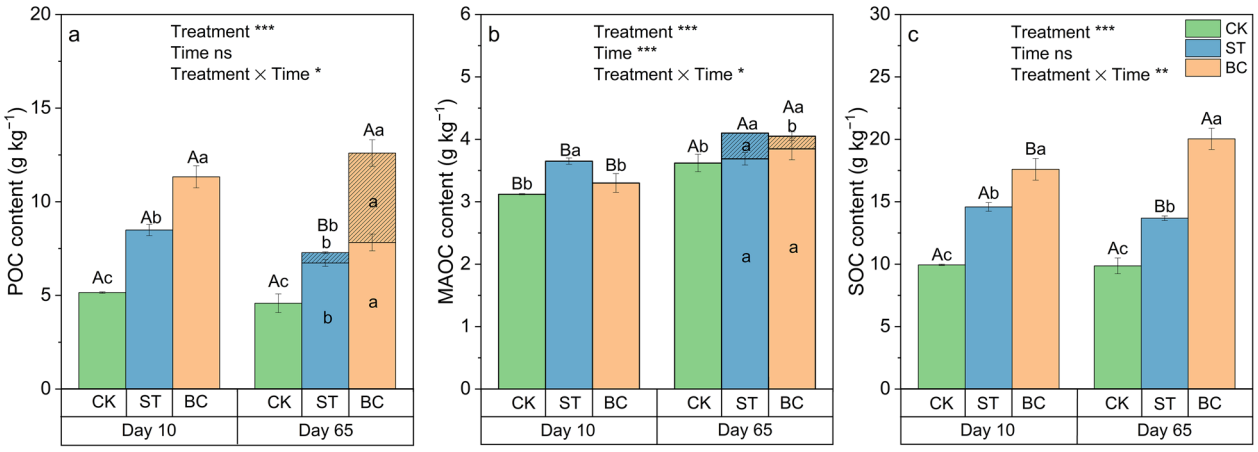


**Fig. 1** Effects of rice straw (ST) and straw-derived biochar (BC) on soil carbon fractions: **a** particulate organic carbon (POC), **b** mineral-associated organic carbon (MAOC), and **c** soil organic carbon (SOC). Lowercase letters indicate significant differences among different treatments at the same sampling time, while uppercase letters indicate significant differences over time within the same treatment. The hatched bars represent the straw/biochar-derived carbon in POC and MAOC, while the solid bars represent the native soil carbon content. Values are the means ± standard deviation ($n = 3$)

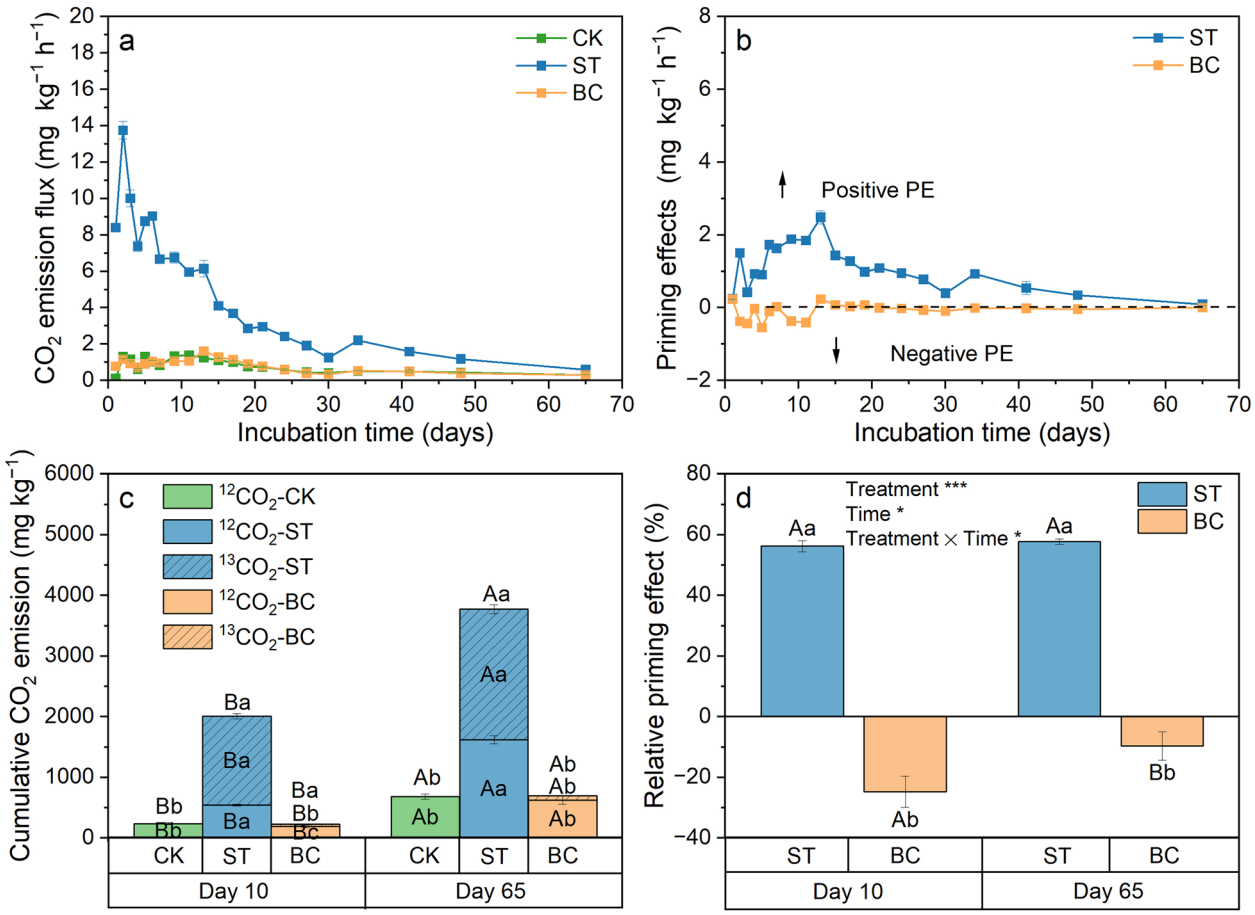


**Fig. 2** Effects of rice straw (ST) and straw-derived biochar (BC) on $CO_2$ emission flux (**a**), priming effect (**b**), cumulative $CO_2$ emission (**c**), and relative priming effect (**d**). Lowercase letters indicate significant differences among different treatments at the same sampling time, while uppercase letters indicate significant differences over time within the same treatment. Values are the means ± standard deviation ($n = 3$)

amendment increased these fractions by 119%, 5.78%, and 77.0%, respectively. Similarly, on day 65, straw amendment led to increases of 58.9% in POC, 13.3% in MAOC, and 38.7% in SOC, while biochar amendment resulted in increases of 174% in POC, 11.9% in MAOC, and 103% in SOC (Fig. 1, $p < 0.05$). Compared with biochar amendment, straw amendment exhibited higher cumulative emissions of total $CO_2$, $^{13}CO_2$, and $^{12}CO_2$ (Fig. 2a, c, $p < 0.05$). Straw induced a positive priming effect, while biochar induced a negative priming effect, which weakened over the course of incubation (Fig. 2b, d).

### 3.2 Effects of straw and biochar on microbial necromass C

After the incubation, compared with the control, straw amendment significantly increased ($p < 0.05$) the contents of MurA, ManN, GalN, GlcN, BNC, FNC, and MNC by 95.5%, 26.5%, 20.8%, 31.5%, 95.5%, 25.4%, and 39.5%, respectively (Table 2). In contrast, biochar amendment significantly increased ($p < 0.05$) MurA,

**Table 2** Effects of straw and straw-derived biochar on soil microbial necromass carbon

| Treatment | MurA (μg g$^{-1}$) | ManN (μg g$^{-1}$) | GalN (μg g$^{-1}$) | GlcN (μg g$^{-1}$) | BNC (mg g$^{-1}$) | FNC (mg g$^{-1}$) | MNC (mg g$^{-1}$) |
|---|---|---|---|---|---|---|---|
| CK | 20.9 ± 2.02c | 19.2 ± 0.88c | 171 ± 22.8b | 326 ± 48.2b | 0.58 ± 0.06c | 2.28 ± 0.35a | 2.86 ± 0.40b |
| ST | 40.9 ± 1.01a | 24.3 ± 0.36a | 206 ± 1.65a | 429 ± 16.8a | 1.13 ± 0.03a | 2.86 ± 0.12a | 3.99 ± 0.15a |
| BC | 28.7 ± 0.34b | 21.9 ± 1.16b | 226 ± 8.67a | 392 ± 27.4ab | 0.80 ± 0.01b | 2.70 ± 0.21a | 3.50 ± 0.21ab |

*CK* control, *ST* straw, *BC* straw-derived biochar. *MurA* Muramic acid, *ManN* Mannosamine, *GalN* Galactosamine, *GlcN* Glucosamine, *BNC* Bacterial necromass carbon, *FNC* Fungal necromass carbon, *MNC* Microbial necromass carbon

**Table 3** Effects of straw and biochar amendment on soil physicochemical properties and enzyme activities

| Treatment | CK | | ST | | BC | | *p* value of two-way ANOVA | | |
|---|---|---|---|---|---|---|---|---|---|
| Time | Day 10 | Day 65 | Day 10 | Day 65 | Day 10 | Day 65 | Treatment | Time | Treatment × Time |
| pH | 6.16 ± 0.07Ab | 6.27 ± 0.01Ac | 6.73 ± 0.13Aa | 6.51 ± 0.01Ab | 6.69 ± 0.11Aa | 6.59 ± 0.04Aa | *** | ns | * |
| DOC (mg $kg^{-1}$) | 81.5 ± 1.41Bc | 96.0 ± 4.60Ab | 115 ± 1.47Aa | 115 ± 5.08Aa | 90.1 ± 0.60Bb | 104 ± 4.71Aab | *** | ** | * |
| MBC (mg $kg^{-1}$) | 23.3 ± 0.64Ab | 17.6 ± 2.01Bb | 59.3 ± 3.64Aa | 39.3 ± 6.64Ba | 26.7 ± 0.98Ab | 25.6 ± 3.37Ab | *** | ** | ** |
| MBN (mg $kg^{-1}$) | 1.25 ± 0.45Bc | 10.6 ± 2.06Aa | 8.63 ± 0.56Aa | 2.75 ± 0.98Bb | 5.97 ± 0.48Ab | 4.24 ± 2.62Ab | ns | ns | *** |
| MBC:MBN ratio | 20.6 ± 5.65Aa | 1.70 ± 0.31Bb | 6.90 ± 0.62Bb | 15.3 ± 3.31Aa | 4.50 ± 0.23Ab | 9.26 ± 6.33Aab | ns | ns | *** |
| TN (g $kg^{-1}$) | 1.22 ± 0.02Ab | 1.18 ± 0.07Ab | 1.40 ± 0.01Ba | 1.51 ± 0.01Aa | 1.38 ± 0.02Ba | 1.51 ± 0.02Aa | *** | ** | ** |
| $NH_4^+$–N (mg $kg^{-1}$) | 9.96 ± 3.72Ab | 7.31 ± 0.61Ab | 12.8 ± 1.46Ab | 11.0 ± 0.66Aa | 42.3 ± 1.64Aa | 12.3 ± 2.16Ba | *** | ** | * |
| $NO_3^-$–N (mg $kg^{-1}$) | 145 ± 3.26Aa | 150 ± 2.58Aa | 59.6 ± 1.09Bc | 77.7 ± 1.24Ac | 104 ± 3.81Bb | 140 ± 2.35Ab | *** | *** | *** |
| BG (nmol $h^{-1}$ $g^{-1}$) | 144 ± 2.05Bb | 174 ± 12.6Ab | 743 ± 17.6Aa | 760 ± 49.6Aa | 128 ± 3.46Bb | 159 ± 14.9Ab | *** | ns | ns |
| NAG (nmol $h^{-1}$ $g^{-1}$) | 92.9 ± 7.41Bb | 180 ± 8.85Ab | 510 ± 17.5Aa | 465 ± 18.62Aa | 96.8 ± 3.44Bb | 133 ± 4.67Ac | *** | ** | *** |
| LAP (nmol $h^{-1}$ $g^{-1}$) | 16.3 ± 3.90Aab | 2.15 ± 0.11Bb | 22.3 ± 3.69Aa | 4.15 ± 0.74Ba | 13.6 ± 1.45Ab | 1.98 ± 0.32Bb | * | *** | ns |
| ACP (nmol $h^{-1}$ $g^{-1}$) | 900 ± 20Bb | 1220 ± 50Ab | 2170 ± 40Aa | 2060 ± 570Aa | 800 ± 30Bc | 1110 ± 50Ab | *** | ns | ns |
| BG/(NAG + LAP) | 1.33 ± 0.12Aab | 0.95 ± 0.03Bb | 1.40 ± 0.06Aa | 1.62 ± 0.12Aa | 1.16 ± 0.04Ab | 1.18 ± 0.15Ab | *** | ns | ** |
| BG/ACP | 0.16 ± 0.00Ab | 0.14 ± 0.02Ab | 0.34 ± 0.01Aa | 0.4 ± 0.13Aa | 0.16 ± 0.01Ab | 0.14 ± 0.02Ab | *** | ns | ns |
| Vector length | 0.59 ± 0.02Ab | 0.5 ± 0.01Bb | 0.64 ± 0.01Aa | 0.68 ± 0.03Aa | 0.55 ± 0.01Ab | 0.55 ± 0.03Ab | ns | *** | ** |
| Vector angle (°) | 76.4 ± 0.39Aa | 75.6 ± 1.11Aa | 66.3 ± 0.68Ab | 65.6 ± 4.75Ab | 75.6 ± 0.74Aa | 76.9 ± 0.71Aa | ns | *** | ns |

*CK* control, *ST* straw, *BC* straw-derived biochar. *DOC* dissolved organic carbon, *MBC* microbial biomass carbon, *MBN* microbial biomass nitrogen, *TN* total nitrogen, *$NH_4^+$–N* ammoniacal nitrogen, *$NO_3^-$–N* nitrate nitrogen, *BG* β-glucosidase, *NAG* β-1,4-N-acetylglucosaminidase, *LAP* leucine aminopeptidase, *ACP* acid phosphatase. Different lowercase letters indicate significant differences among treatments within the same sampling time ($p < 0.05$). Different uppercase letters indicate significant differences between sampling times (day 10 vs. day 65) within the same treatment ($p < 0.05$). Asterisks (*, **, ***) indicate significant effects at $p < 0.05$, $p < 0.01$, and $p < 0.001$, respectively, based on two-way ANOVA. 'ns' indicates no significant effect ($p \geq 0.05$)

ManN, GalN, and BNC by 37.3%, 14.2%, 32.2%, and 37.3%, respectively, but had no significant effects on GlcN, FNC, and MNC.

### 3.3 Effects of straw and biochar on soil physicochemical properties and enzyme activities

Treatment type, sampling time, and their interaction significantly ($p < 0.05$) affected soil physicochemical properties and enzyme activities (Table 3). Throughout the incubation period, compared with the control, straw amendment increased ($p < 0.05$) soil pH (3.80–9.40%), DOC (19.5–40.8%), MBC (124–155%), and TN (14.8–28.6%) contents, while biochar amendment increased ($p < 0.05$) soil pH (5.10–8.66%), $NH_4^+$–N (68.6–324%), and TN contents (13.1–30.6%). Both straw and biochar amendment reduced $NO_3^-$–N concentrations. Notably, the MBN content increased significantly ($p < 0.05$) on the 10th day under both straw (590%) and biochar amendment (377%), but decreased ($p < 0.05$) on the 65th day by − 74.2% and − 60.2%, respectively.

Compared with the control, straw amendment enhanced the activities of BG (337–416%), NAG (158–449%), LAP (37.3–92.9%), and ACP (68.7–140%) enzymes. Conversely, biochar amendment reduced ACP activity (−11.3%) on the 10th day and suppressed NAG activity (−26.2%) on the 65th day. Compared with the control, straw amendment significantly increased ($p < 0.05$) the BG/ACP ratio and vector length, while decreasing vector angle; however, no significant changes were observed under biochar amendment.

### 3.4 Effects of straw and biochar on soil microbial life-history strategies

Compared with the control, straw amendment significantly reduced the bacterial Chao richness index and Shannon diversity index (Fig. S1, $p < 0.05$). Principal component analysis (PCA) of β-diversity demonstrated that the first two principal components explained 33.8% (day 10) and 30.3% (day 65) of the total variance in bacterial communities, and 37.6% and 35.4% of that in fungal communities (Fig. 3). By day 65, PCA revealed clear separation of bacterial and fungal communities across all treatment groups.

Straw amendment enhanced the relative abundance of Mortierellomycota and Actinobacteriota while reducing the relative abundances of Proteobacteria, Ascomycota, Acidobacteriota, Chloroflexi, and Basidiomycota, thereby influencing both r- and *K*-strategist microorganisms (Fig. S2; Fig. 4, $p < 0.05$). Although biochar did not induce significant shifts in microbial composition compared to the control, it notably enhanced the relative abundances of *K*-strategist microorganisms (e.g., Actinobacteriota, Chloroflexi, and Basidiomycota) compared to straw amendment by the end of the incubation period.

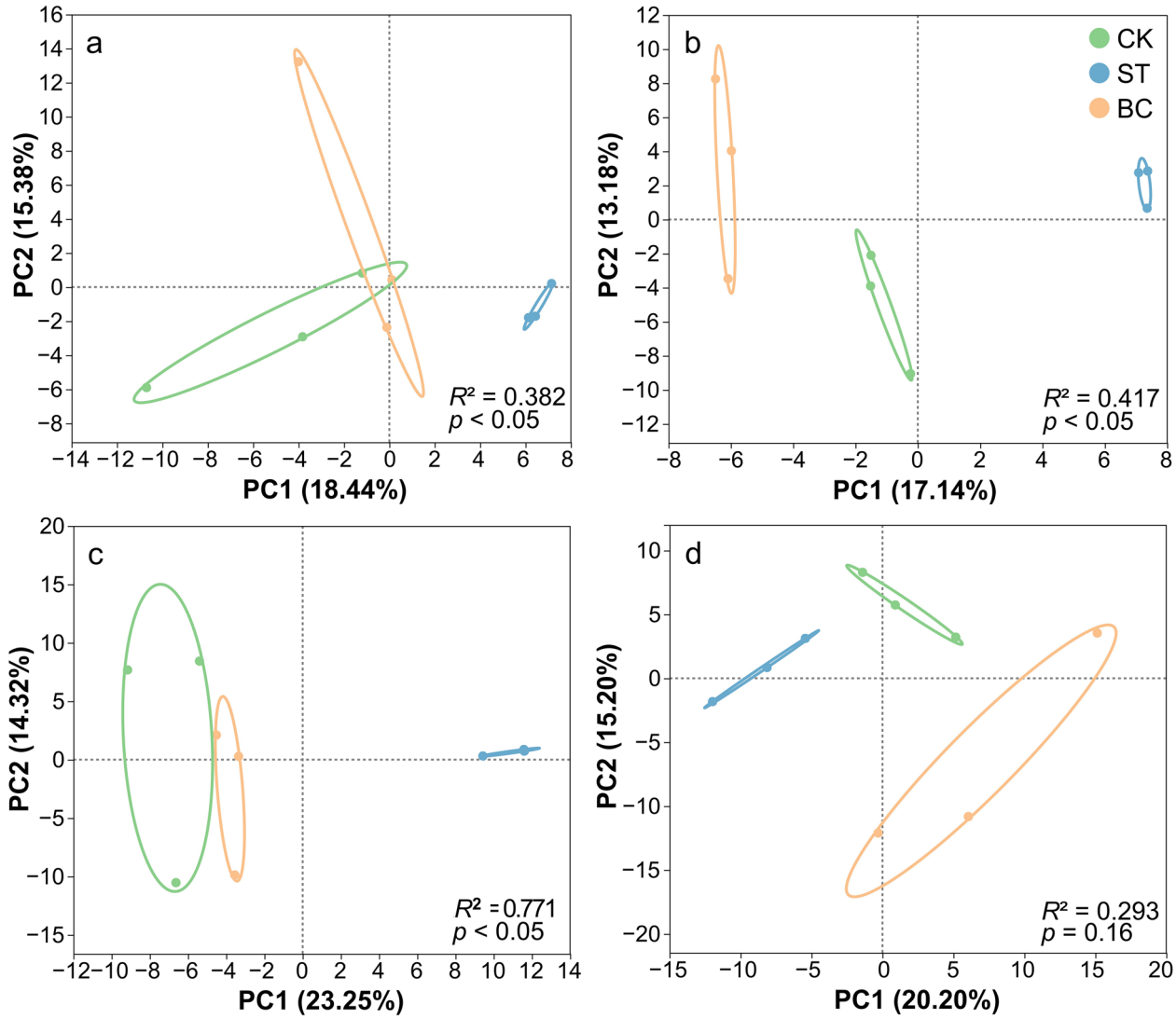


**Fig. 3** Principal component analysis (PCA) of the bacterial and fungal communities. The $R^2$ and $p$ values in the figure are the results of PERMANOVA analysis. PCA results for the bacterial communities on day 10 and 65 are shown in **a** and **b**, respectively, while those for the fungal communities are shown in **c** and **d**, respectively

### 3.5 Key factors influencing SOC fractions after straw and biochar amendment

Mantel test analyses demonstrated positive correlations between SOC fractions and soil physicochemical properties (e.g., MBC, pH, DOC, TN), microbial life-history strategies, and enzyme activities (e.g., NAG, ACP) under straw amendment (Fig. 5a). In contrast, under biochar amendment, SOC fractions were primarily associated with soil properties (e.g., MBC, pH, TN, $NO_3^-$–N) (Fig. 5b). Correlation analysis showed that after straw amendment, NAG was positively ($p < 0.05$) correlated with MBC, pH, DOC, TN, Firmicutes, Mortierellomycota, etc., and negatively ($p < 0.05$) correlated with $NO_3^-$–N, Chloroflexi, Proteobacteria, etc. ACP was positively ($p < 0.05$) correlated with MBC, pH, DOC, TN, Mortierellomycota, etc., and negatively ($p < 0.05$) correlated with $NO_3^-$–N, Proteobacteria, Basidiomycota, etc. After biochar amendment, LAP was positively ($p < 0.05$) correlated with Acidobacteriota, Proteobacteria, etc., and negatively ($p < 0.05$) correlated with DOC, Chloroflexi, etc.

Random forest modeling further elucidated the key predictors governing different C fractions. Under straw amendment, POC and SOC dynamics were predominantly influenced by key physicochemical properties (e.g., DOC, MBC, pH) and enzyme activities (e.g., ACP,

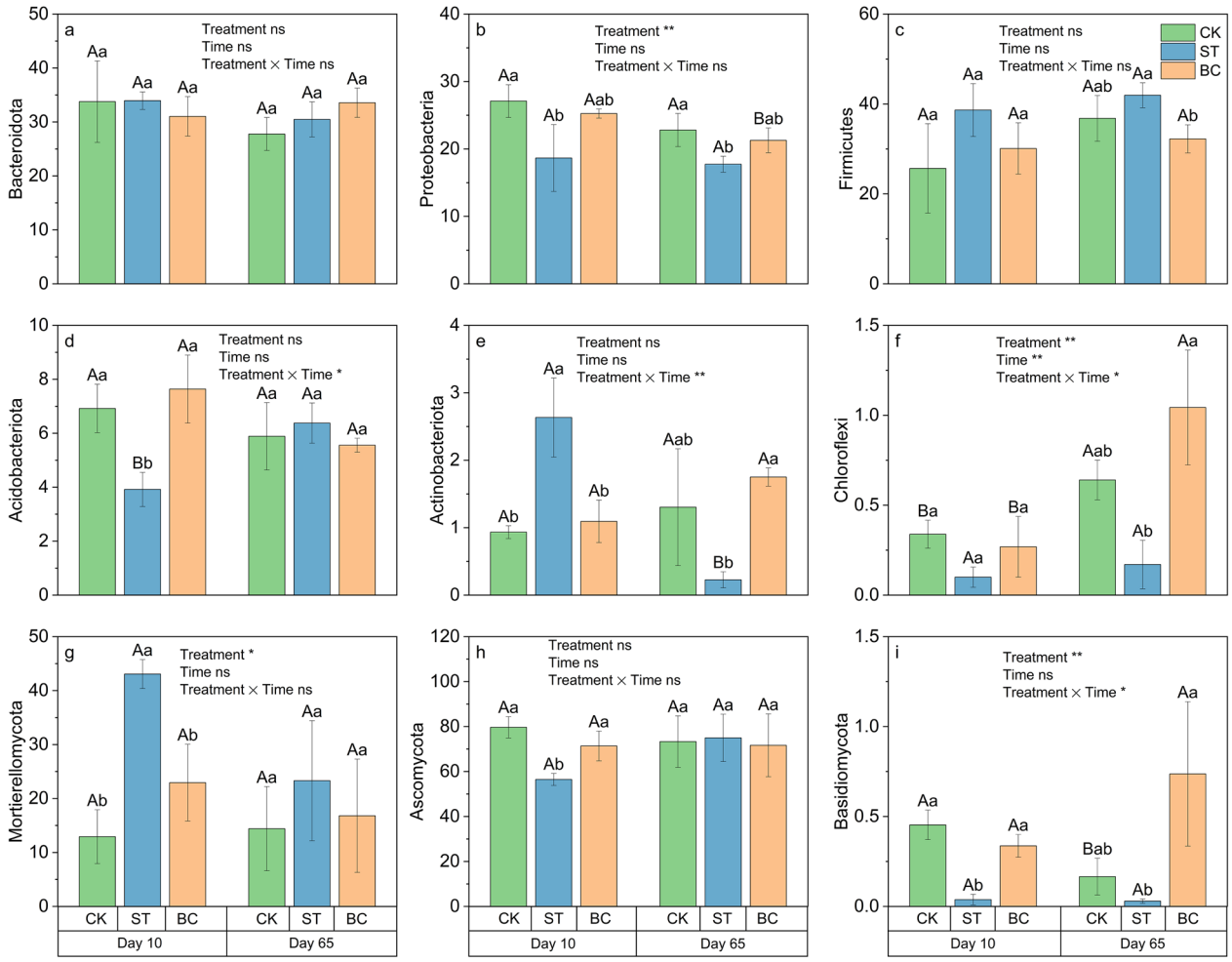


**Fig. 4** Effects of rice straw and straw-derived biochar on microbial life-history strategies. Bacterial r-strategists are shown in **a**, **b**, and **c**; bacterial *K*-strategists in **d**, **e**, and **f**; fungal r-strategists in **g** and **h**; and fungal *K*-strategists in **i**. Lowercase letters indicate significant differences among different treatments at the same sampling time, while uppercase letters indicate significant differences over time within the same treatment. Values are the means ± standard deviation ($n = 3$)

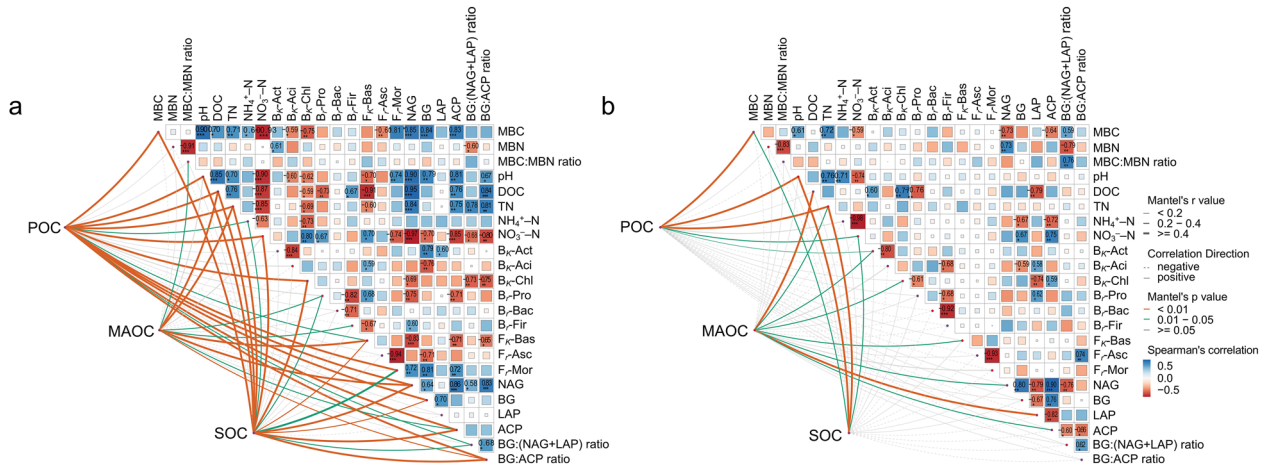


**Fig. 5** Correlations between environmental variables, microbial life-history strategies, enzyme activities and POC, MAOC, and SOC under rice straw (**a**) and straw-derived biochar (**b**) treatments

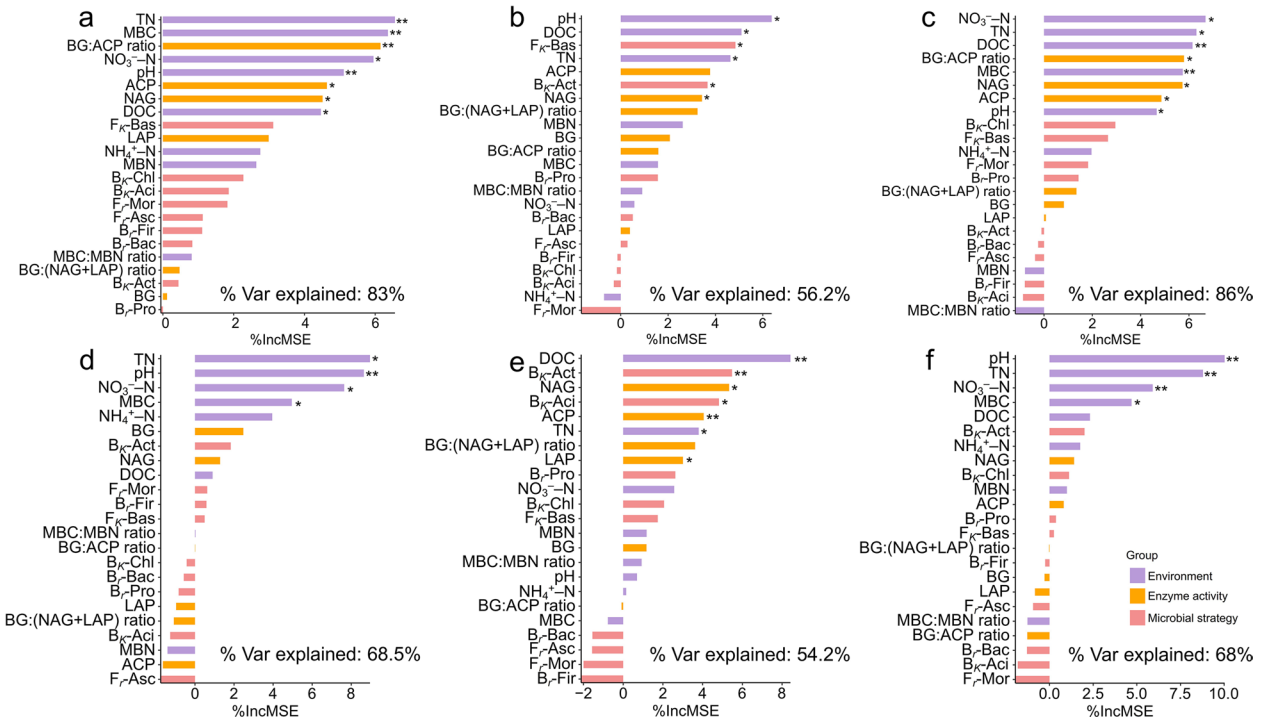


**Fig. 6** Random forest analysis to identify the relative importance of predictors for the responses of POC, MAOC, and SOC. The relative importance for POC, MAOC, and SOC following rice straw amendment is shown in **a**, **b**, and **c**, respectively, and following straw-derived biochar amendment in **d**, **e**, and **f**, respectively. Mean squared errors (MSE) show the importance of each predictor. The symbols *, **, and *** indicate significant differences at $p < 0.05$, $p < 0.01$, and $p < 0.001$, respectively

NAG), which were identified as the critical factors. For MAOC under straw amendment, predictive factors further encompassed specific microbial taxa such as Basidiomycota and Actinobacteriota, in addition to certain physicochemical parameters (Fig. 6a). Notably, this random forest model explained 56.2% of the total variance. Following biochar amendment, the key factors influencing POC and SOC were primarily soil physicochemical properties such as pH, MBC, and TN. Regarding MAOC under biochar amendment, in addition to physicochemical properties (DOC and TN), key influencing factors included enzyme activities (NAG and ACP) and microbial groups (e.g., Actinobacteriota and Acidobacteriota) (Fig. 6b). This pattern suggests that *K*-strategist microbes serve as key predictors for MAOC dynamics, whereas changes in POC and SOC are mainly governed by physicochemical factors.

### 3.6 Straw and biochar amendment affect SOC via distinct pathways

After straw amendment, the SEM explained 89% of total SOC content (Fig. 7a), and POC contributed more to SOC than MAOC. The results showed that DOC directly and indirectly promotes the accumulation of POC (via ACP and Mortierellomycota) and MAOC (via NAG and Firmicutes). Standardized path coefficients showed that DOC had the greatest total effect on POC, MAOC, and SOC, with standardized path coefficients of 0.78, 0.84, and 0.85, respectively ($p < 0.01$, Fig. 7b).

The SEM explained 91% of SOC content under biochar amendment, in which POC made a greater contribution to SOC than MAOC (Fig. 7c). Acting as key drivers of SOC increase, DOC and MBC directly and positively affect POC. DOC and MBC influence MAOC, and consequently SOC increase, by modulating LAP activity, Actinobacteriota, and Chloroflexi. Specifically, MBC and LAP activity exert negative effects on MAOC (path coefficients of −0.22 and −0.61, respectively), whereas DOC, Actinobacteriota, and Chloroflexi have positive effects (path coefficients of 0.49, 0.50, and 0.50, respectively, Fig. 7d).

### 3.7 Effects of straw and biochar on net C balance and C sequestration efficiency

Treatment type, sampling time, and their interaction significantly affected soil net C balance and C sequestration efficiency (Fig. 8, $p < 0.001$). During the incubation period, both the net C balance and C sequestration efficiency of biochar amendment were higher than those of straw amendment ($p < 0.05$). Compared

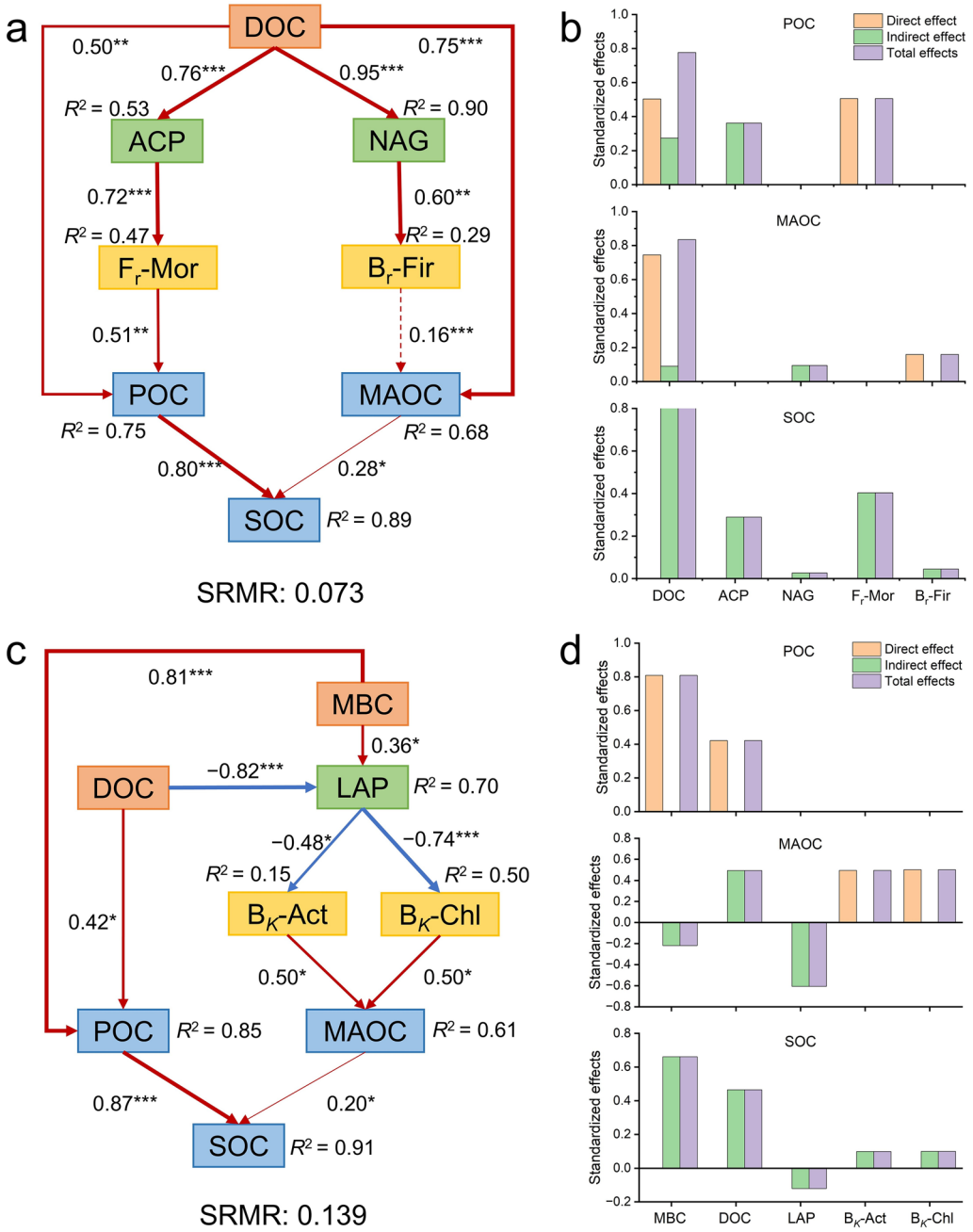


**Fig. 7** Structural equation modeling (SEM) illustrating the effects of rice straw (**a**) and straw-derived biochar (**c**) amendment on POC, MAOC, and SOC. Significant paths are shown in red lines if positive or in blue lines if negative. The numbers above lines are the standardized path coefficients. The symbols *, **, and *** denote significance at $p < 0.05$, $p < 0.01$, and $p < 0.001$, respectively. The variance explained ($R^2$) by the SEM for each response variable is shown. **b** and **d** show the standardized direct, indirect, and total effects of different factors on POC, MAOC, and SOC following rice straw and straw-derived biochar amendment, respectively

with straw amendment, biochar amendment increased ($p < 0.05$) the net C balance by 79.9% and 338% at 10 and 65 days of incubation, respectively. As the incubation time extended, the net C balance and C sequestration efficiency of straw amendment gradually decreased, whereas biochar amendment showed no significant changes. At 10 days, the C sequestration efficiencies for straw and biochar amendments were 55.7% and 100%,

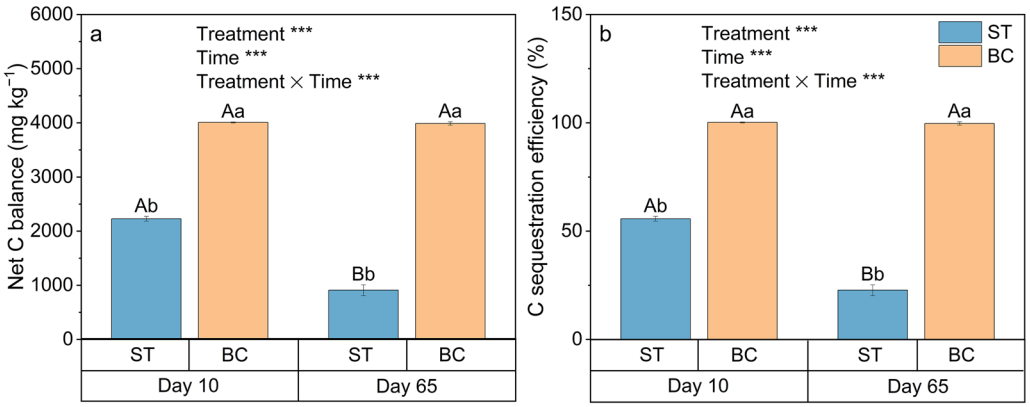


**Fig. 8** Effects of straw (ST) and straw-derived biochar (BC) on net C balance (**a**) and C sequestration efficiency (**b**). Lowercase letters indicate significant differences among different treatments at the same sampling time, while uppercase letters indicate significant differences over time within the same treatment. Values are the means ± standard deviation ($n = 3$)

respectively; at 65 days, they were 22.8% and 99.7%, respectively.

## 4 Discussion

### 4.1 Positive priming by straw and negative priming by biochar drive differential C turnover

The distinct SOC sequestration capacities of straw and biochar amendments are fundamentally linked to their contrasting effects on microbial priming and native C loss, representing a critical trade-off. Straw amendment introduces readily decomposable C, providing an excess energy substrate for microorganisms (Xie et al. 2025). Compared with the control, the vector length and the ratios of BG/(NAG + LAP) and BG/ACP were significantly higher in the straw amendment (Table 3), indicating enhanced microbial investment in C acquisition relative to nitrogen and phosphorus acquisition. Higher cumulative emissions of $CO_2$, $^{13}CO_2$, and $^{12}CO_2$ in the straw amendment compared to the biochar amendment (Figs. 2a, c) were attributed to the rapid decomposition of straw and its promotion of hydrolytic enzyme activities (BG, NAG, LAP, ACP), which accelerated the turnover of native C (notably POC), thereby inducing a strong positive priming effect (Table 3, Fig. 1). This suggests that the high-energy input of straw triggered a co-metabolism effect, where microbes utilized the labile energy to mine recalcitrant soil organic matter for nutrients (nitrogen mining), resulting in a net cost to the native C stock (Chen et al. 2014; Fu et al. 2025). Moreover, a portion of the POC increase under straw amendment consists of undecomposed or partially decomposed straw fragments that may be physically protected within soil aggregates (Fig. 1a). Although temporarily retained in the POC pool, this material remains labile and is susceptible to mineralization over longer timescales, particularly when aggregates are disrupted or under changing environmental conditions (Yang et al. 2025a). Thus, this physically protected but undecomposed straw C represents transient C accumulation rather than true long-term stabilization. Therefore, although the SOC and POC content generally increased after straw amendment (Fig. 1), this increase was partially offset by an accelerated loss of native C, resulting in a considerably lower net C balance and C sequestration efficiency in the straw amendment compared to the biochar amendment (Fig. 8).

Conversely, biochar amendment induced a negative priming effect, a phenomenon likely resulting from mechanisms such as physical protection and altered microbial functioning that reduce native SOC mineralization. Biochar possesses a highly aromatic and recalcitrant structure (Lehmann et al. 2006). Its porosity and strong adsorption capacity may promote soil aggregation via particle cementation, forming stable aggregates that may act as a physical barrier to protect both native and newly added C by limiting microbial-substrate contact (Han et al. 2020; Okebalama and Marschner 2023). The results showed that biochar significantly increased POC content (174%), with a substantial portion originating from native soil C (Fig. 1a), suggesting that the organic matter may have been physically protected by aggregates. However, we acknowledge that without direct measurements of aggregates, this remains an inference rather than a confirmed mechanism. After biochar amendment, the activities of nitrogen-acquiring enzymes such as LAP decreased significantly (Table 3). This is consistent with previous studies (Bailey et al. 2011; Barthod et al. 2016; Hu et al. 2023; Yang et al. 2025c), which have shown that biochar reduces enzyme–substrate contact through adsorption and temporarily inhibits microbial activity

due to its alkalinity, thereby decreasing the production of hydrolytic enzymes (e.g., phosphatases, chitinases) and slowing organic C mineralization. Together, these mechanisms suppress the decomposition of native SOC, enhance the retention of biochar-derived recalcitrant C, and facilitate the incorporation of newly added C into the POC pool, thereby collectively promoting SOC sequestration (Figs. 1, 2, 8). Research confirms the high stability of biochar-derived C in soil, with 74% recovered in the free light fraction after 10 months in temperate forest soil (Singh et al. 2014; Wang et al. 2022). Substantial evidence indicates that biochar amendment results in higher $^{13}C$ contribution percentages and increased contents of total SOC, POC, and MAOC (Yang et al. 2025a). This stability explains why the biochar amendment led to a much greater increase in POC (174%) and a much higher C sequestration efficiency (99.7%) compared to the straw amendment (58.9% and 22.8%, respectively) by the end of the incubation.

### 4.2 The regulatory role of r-strategists on POC and MAOC under straw amendment

Bacterial and fungal life-history strategies were categorized at the phylum level. For bacteria, phyla including Bacteroidota, Firmicutes, and Proteobacteria were classified as r-strategist (copiotrophic), while Actinobacteriota, Acidobacteriota, and Chloroflexi were designated as *K*-strategist (oligotrophic) (Fierer et al. 2007; Francioli et al. 2016; Nemergut et al. 2010; Phung et al. 2004). Among fungi, Ascomycota and Mortierellomycota were assigned to the r-strategist group, and Basidiomycota was categorized as a *K*-strategist phylum (Wu et al. 2021; Yao et al. 2017).

During straw decomposition, readily utilizable substrates such as cellulose and hemicellulose are released, providing a competitive advantage to fast-growing r-strategists (e.g., Firmicutes and Mortierellomycota) (Fig. 7) (Wu et al. 2025). This resulted in a significant decrease in soil bacterial Chao richness and Shannon diversity, which was attributed to competitive exclusion of other microorganisms by rapidly proliferating r-strategists (Fig. S1) (Hammarlund et al. 2019; Zhang et al. 2018). The enrichment of r-strategist microbes regulates the specific trade-off in C allocation between the POC and MAOC fractions. For the biochar amendment, although the increase in soil pH (Table 3) may independently affect community diversity by favoring alkaliphilic groups over acidophilic groups, the absence of readily available C sources and the provision of a stable microhabitat through dynamic regulation of soil moisture and aeration mean that it does not trigger the intense resource competition observed under straw treatment (Yang et al. 2022).

The r-strategist microorganisms regulate POC primarily via fungus-mediated processes. As a typical r-strategist fungus, Mortierellomycota may stabilize soil aggregates by encasing organic fragments with its hyphae, thereby protecting incompletely decomposed straw C within the POC pool from rapid mineralization (Li et al. 2023; Song et al. 2024). This physical protection mechanism, combined with the significant increase in FNC observed under straw amendment (Table 2), suggests that Mortierellomycota may contributes to both aggregate formation and necromass-mediated C stabilization. SEM results demonstrate a strong positive effect of Mortierellomycota on POC (with a path coefficient of 0.51, $p < 0.01$), consistent with this mechanism. Nevertheless, the link between Mortierellomycota and aggregate formation in our specific experimental system remains to be empirically verified. Furthermore, this observed enhancement in fungal abundance and activity was primarily driven by increased DOC and ACP activity. The significant positive correlation between ACP activity and the relative abundance of Mortierellomycota (Fig. 5) suggests that phosphorus availability may play a critical role in fungal-mediated C sequestration under straw amendment. Following straw amendment, the increase in ACP activity (Table 3) and the reduction in vector angle collectively indicated a marked alleviation of soil phosphorus limitation. This alleviation likely promoted microbially mediated C stabilization processes and created favorable edaphic conditions for the subsequent proliferation of Mortierellomycota. These findings align with previous research demonstrating that the application of chemical phosphorus fertilizer to soils with a long-term history of phosphorus deficiency significantly enriches Mortierellomycota populations (Yang et al. 2025b).

Under straw amendment, DOC, enzyme activities, and microbial taxa form a coordinated ecological network. The results indicate a significant positive correlation between NAG activity and both DOC and Firmicutes (Fig. 5a), suggesting that DOC may influence the proliferation of Firmicutes by regulating nitrogen-acquiring enzyme activities. Specifically, the DOC released during straw decomposition provides readily available C sources and energy for microorganisms, while simultaneously inducing the expression of nitrogen-acquiring enzymes (e.g., NAG) by stimulating microbial demand for nitrogen (Table 3). For r-strategist bacteria such as Firmicutes, which are highly sensitive to fluctuations in carbon and nitrogen substrates (Grant et al. 2022), the enhanced availability of organic nitrogen resulting from increased NAG activity likely directly promotes their rapid growth and proliferation (Figs. 4c, 5a). Although the direct pathway from Firmicutes to MAOC did not reach statistical significance, Firmicutes may indirectly

contribute to MAOC formation through the accumulation of necromass following their rapid growth and death (Table 2). Studies have shown that in research combining green manure with straw amendment, several bacterial genera within the phylum Firmicutes were significantly positively correlated with bacterial necromass C (Zhou et al. 2025a). In a $^{13}CO_2$-labeled rhizo-box experiment, the abundance of Firmicutes was found to be significantly positively correlated with $^{13}$C-MAOC (Han et al. 2025). Thus, this observation directly confirms our initial hypothesis: straw amendment enhances both POC and MAOC accumulation by enriching r-strategist microorganisms, whereby fungal (Mortierellomycota) and bacterial (Firmicutes) r-strategists differentially drive C stabilization—the former possibly through aggregate-mediated POC protection and the latter through necromass-driven MAOC accrual.

Although straw amendment increased the contents of both POC and MAOC, the positive priming effect indicated a significant net C loss, particularly due to the rapid mineralization of the POC pool (Figs. 1, 2) (Fu et al. 2025). This is primarily associated with the conversion of straw-derived $^{13}$C from POC to MAOC (Chaudhary et al. 2014). Therefore, r-strategist microbes rapidly utilize straw-derived labile POC for energy acquisition. While this feasting strategy accelerates the microbial C pump and generates substantial necromass (contributing to MAOC), the low C use efficiency (CUE) typically associated with r-strategists means that a large proportion of C is respired as $CO_2$ (Chen et al. 2016). This explains why straw amendment resulted in lower C sequestration efficiency despite high microbial activity (Fig. 8).

### 4.3 The regulatory role of *K*-strategists on POC and MAOC under biochar amendment

Biochar amendment promotes C sequestration by altering soil physicochemical properties and enriching slow-growing *K*-strategist microorganisms (Shang et al. 2023). By dynamically regulating soil moisture and aeration, biochar creates a stable microhabitat for microorganisms, avoiding the dramatic community fluctuations induced by straw amendment (Yang et al. 2022). Consequently, the biochar amendment showed no significant effect on microbial α-diversity (Fig. S1). After 65 days of incubation, compared with the control, the POC content in biochar-amended soils increased significantly by 174%—a magnitude far greater than the 58.9% increase observed in straw-amended soils (Fig. 1). Notably, the elevated POC under biochar amendment comprised two distinct fractions: biochar-derived C and native soil-derived C (Fig. 1a). This dual-source origin suggests that the observed POC accumulation stems from two complementary mechanisms: (1) direct physical protection provided by biochar particles themselves, whose highly aromatic and recalcitrant molecular structure inherently resists decomposition (Lehmann et al. 2006); and (2) the formation of newly stabilized soil-derived organic matter, likely facilitated by biochar-induced soil aggregate formation. The substantial contribution of native soil C to the POC pool indicates that biochar acts as a binding agent, cementing soil particles and organic fragments into stable macroaggregates that physically protect native organic matter from microbial degradation (Han et al. 2020; Okebalama and Marschner 2023).

Biochar's regulation of MAOC formation primarily relies on metabolic resource reallocation by *K*-strategist microorganisms. Specifically, biochar's adsorption of $NH_4^+$–N reduces soil nitrogen bioavailability, thereby lowering microbial nitrogen demand. This physiological response is reflected by the decreased LAP activity observed in biochar treatments (Table 3), indicating that microorganisms reduce energy and material investment in nitrogen mineralization pathways. By reallocating metabolic resources away from nitrogen acquisition, microbes can divert more energy toward transforming recalcitrant aromatic C (e.g., aromatic hydrocarbons) present in biochar (Nordmeyer and Richter 1985; Wang et al. 2025a). Slow-growing *K*-strategists (e.g., Actinobacteriota and Chloroflexi), which are selectively enriched under these nitrogen-limited conditions, likely exhibit higher CUE. Consistent with this, previous studies have demonstrated that microbial CUE increases with the relative abundance of *K*-strategists compared to r-strategists, with CUE being significantly higher during the decomposition phase dominated by *K*-strategists than that by r-strategists. We further propose that the prevalence of *K*-strategists represents a key microbial mechanism driving high CUE (Ma et al. 2023). By allocating more resources to cellular biomass synthesis rather than respiration energy loss, these oligotrophic taxa efficiently convert recalcitrant biochar-C into stable microbial necromass, thereby promoting MAOC formation without inducing substantial respiratory losses (Table 2) (Liu et al. 2023; Zhang et al. 2024a).

SEM results revealed that DOC and MBC in biochar-amended soils indirectly regulated MAOC formation through two pathways: modulating LAP activity to alter microbial resource allocation, and interacting with *K*-strategists, where both Actinobacteriota and Chloroflexi exhibited strong positive path coefficients (0.50) toward MAOC (Fig. 7). These findings are supported by an 11-year long-term field experiment, which showed that combined biochar and nitrogen fertilizer application significantly increased Actinobacteria abundance, which was positively correlated with microbial necromass

C—itself strongly associated with elevated MAOC content (Zhang et al. 2024a). Additionally, Liu et al. (2025b) reported that multiple key genera within Actinobacteria phylum were positively correlated with a suite of soil C stability indicators, further validating the role of *K*-strategists in MAOC stabilization.

Furthermore, the increased soil pH (by 5.10–8.66%) induced by biochar improves the habitat suitability for *K*-strategist microorganisms. Simultaneously, the adsorbed DOC and low-molecular-weight organic compounds provide these microbes with a sustained C supply, ensuring the stable production of microbial necromass (Smith et al. 2010).

Notably, while the magnitude of MAOC accumulation under biochar amendment was lower than that of POC, the strong physicochemical binding between microbial necromass and soil mineral surfaces endows *K*-strategist-mediated MAOC with greater stability. These findings directly validate our initial our hypothesis that biochar promotes MAOC formation by selectively enriching *K*-strategist microbes (e.g., Actinobacteriota and Chloroflexi), which efficiently convert recalcitrant biochar-derived C into stable microbial necromass that persists in mineral-associated pools.

### 4.4 Effects of temporal dynamics on SOC fractions and C sequestration under straw and biochar amendment

This study found that from day 10 to day 65, the POC content in straw-amended soils slightly decreased from an initial increase of 64.7% to 58.9%, while the MAOC content also declined from an increase of 17.0% to 13.3% (Fig. 1). These results indicate that the positive priming effect induced by straw input gradually weakened the net C accumulation during the later stage of incubation. This phenomenon can be attributed to the time-dependent nature of the "co-metabolism" mechanism during straw decomposition. In the early stage, the release of abundant readily decomposable organic matter stimulates intensive microbial growth. However, as the available C source is depleted, microbial activity declines, and a portion of the initially stabilized POC may be mineralized or transformed into MAOC (Chaudhary et al. 2014; Fu et al. 2025). Consistent with this, the net C balance under straw amendment decreased significantly from day 10 to day 65, with C sequestration efficiency dropping from 55.7% to 22.8% (Fig. 8). These findings suggest that C accumulation following straw input is highly dynamic over time, and short-term sequestration effects are difficult to sustain.

In contrast, the POC content, net C balance, and C sequestration efficiency under biochar amendment remained nearly unchanged throughout the 65-day incubation period, demonstrating temporal stability (Fig. 8). Kuzyakov et al. (2009) suggested that the mean residence time of biochar in soil is approximately 2000 years, with only about 0.5% decomposing annually. From this perspective, the 65-day incubation period in this study represents a relatively short window for assessing the long-term behavior of biochar, which imposes certain limitations. Therefore, while our findings demonstrate the potential of biochar to initiate mechanisms favorable for SOC sequestration, confirmation of its long-term sequestration efficacy requires multi-year to decadal observations. It is worth noting that although biochar exhibited a negative priming effect within the 65-day period (Fig. 2), in the long term, as the biochar surface becomes colonized by microorganisms, the priming effect may undergo complex dynamic changes. A meta-analysis of 1170 data pairs from 27 incubation studies found that the priming effect following biochar amendment was initially negative within 0–206 days, turned positive and peaked at around 773 days, and then returned to negative in the later stage (Ding et al. 2018). A ten-year field study in subtropical grassland found that a negative priming effect was still detectable a decade after biochar amendment, indicating its long-term protective effect on SOC (Weng et al. 2017). Thus, while the negative priming observed at day 65 aligns with short-term patterns, the trajectory may evolve over longer timescales—potentially shifting toward positive priming before returning to negative priming. Future studies with extended incubation periods are needed to validate this proposed trajectory under our specific experimental conditions.

We acknowledge that the lack of sampling points between days 10 and 65 limits our ability to capture the full temporal dynamics of microbial community succession under biochar amendment. However, based on the existing literature, we can infer the expected trajectory. The initial stage (days 0–10) is likely dominated by r-strategist microorganisms utilizing the labile C fraction associated with fresh biochar (Yu et al. 2018). As this labile pool becomes depleted, a gradual transition toward *K*-strategist dominance is expected to occur between days 10 and 40 (Liu et al. 2025a; Yu et al. 2018). By day 65, the community reaches a *K*-strategist-dominated equilibrium, as observed in our study (Fig. 3). This succession pattern is consistent with long-term observations showing that biochar-induced shifts toward oligotrophic taxa become more pronounced over time as the system stabilizes (Huang et al. 2024). Future studies with higher temporal resolution sampling—particularly during the critical transition window between days 10 and 40—would help validate this proposed trajectory and elucidate the specific microbial taxa driving the succession.

## 5 Conclusions

Both straw and biochar amendments enhanced the SOC sequestration. Straw amendment supplies readily decomposable C, which stimulates hydrolytic enzyme activity and enriches r-strategist microorganisms (e.g., Mortierellomycota and Firmicutes). This process promotes the formation of fungus-mediated POC and the accumulation of bacterial necromass-derived MAOC. However, it induced a positive priming effect, accelerated the mineralization of native SOC, and limited the C sequestration efficiency. Biochar induced a negative priming effect and alleviated microbial nitrogen demand, shifting microbial activity toward the decomposition of recalcitrant C, while enriching *K*-strategist microorganisms (such as Actinobacteriota and Chloroflexi). These changes promoted the accumulation of MAOC through the formation of microbial necromass, ultimately achieving high C sequestration efficiency and low C loss. These complementary mechanisms suggest that in agricultural practice, co-application straw with biochar amendment may simultaneously activate multiple C sequestration pathways.

## Supplementary Information

The online version contains supplementary material available at https://doi.org/10.1007/s42773-026-00630-y.

Additional file 1: Fig. S1. Effects of rice straw (ST) and straw-derived biochar (BC) on α-diversity indices. Fig. S2. Effects of straw and biochar on microbial community composition.

**Acknowledgements**
We value constructive feedback from the editors and reviewers.

**Authors contributions**
Liping Na: Data curation, Investigation, Methodology, Visualization, Writing – original draft. Yalin Liu: Visualization, Writing – review & editing. Qiong Nan: Data curation, Formal analysis, Writing – review & editing. Litian Chen: Resources, Methodology. Da Dong: Software. Weixiang Wu: Methodology. Jiangwu Tang: Funding acquisition. Shengmao Yang: Resources. Yuxue Liu: Conceptualization, Project administration, Funding acquisition, Supervision, Writing – review & editing. All authors read and approved the final manuscript.

**Funding**
This research was financially supported by the Zhejiang Province Science and Technology Plan (2025C02267), the Key Science and Technology Research and Development Project of Hangzhou (2024SZD1B24), and the National Natural Science Foundation of China (42077090).

**Data availability**
Data will be shared upon reasonable request.

## Declarations

**Competing interests**
The authors declare no competing interests.

**Author details**
[1]State Key Laboratory for Quality and Safety of Agro-Products, Institute of Environment Resource Soil and Fertilizer, Zhejiang Academy of Agricultural Sciences, Hangzhou 310021, China. [2]International Science and Technology Cooperation Base for the Regulation of Soil Biological Functions and One Health of Zhejiang Province, Ningbo University, Ningbo 315211, China. [3]College of Environment and Resource Science, Zhejiang University, Hangzhou 310058, China. [4]College of Carbon Neutrality, College of Environmental and Resource Sciences, Zhejiang A & F University, Hangzhou 311300, China. [5]Engineering Research Center of Biochar of Zhejiang Province, Hangzhou 310021, China. [6]Zhejiang-UK Joint Laboratory On Soil Health and Agri-Product Safety, Hangzhou 310021, China.

**Received: 22 December 2025 Revised: 4 April 2026 Accepted: 28 April 2026**
Published online: 25 June 2026

**References**

Bailey VL, Fansler SJ, Smith JL et al (2011) Reconciling apparent variability in effects of biochar amendment on soil enzyme activities by assay optimization. Soil Biol Biochem 43(2):296–301. https://doi.org/10.1016/j.soilbio.2010.10.014

Bao SD (2000) Soil and agricultural chemistry analysis. China Agriculture Press, Beijing, pp 263–270

Barthod J, Rumpel C, Paradelo R et al (2016) The effects of worms, clay and biochar on $CO_2$ emissions during production and soil application of composts. Soil 2(4):673–683. https://doi.org/10.5194/soil-2-673-2016

Beillouin D, Corbeels M, Demenois J et al (2023) A global meta-analysis of soil organic carbon in the Anthropocene. Nat Commun 14(1):3700. https://doi.org/10.1038/s41467-023-39338-z

Bray RH, Kurtz LT (1945) Determination of total, organic, and available forms of phosphorus in soils. Soil Sci 59:39–46. https://doi.org/10.1097/00010694-194501000-00006

Brookes PC, Landman A, Pruden G et al (1985) Chloroform fumigation and the release of soil nitrogen: a rapid direct extraction method to measure microbial biomass nitrogen in soil. Soil Biol Biochem 17(6):837–842. https://doi.org/10.1016/0038-0717(85)90144-0

Cambardella CA, Elliott ET (1992) Particulate soil organic-matter changes across a grassland cultivation sequence. Soil Sci Soc Am J 56(3):777–783. https://doi.org/10.2136/sssaj1992.03615995005600030017x

Chaudhary DR, Saxena J, Dick RP (2014) Fate of carbon in water-stable aggregates during decomposition of $^{13}$C-labeled corn straw. Commun Soil Sci Plant Anal 45(14):1906–1917. https://doi.org/10.1080/00103624.2014.909834

Chen RR, Senbayram M, Blagodatsky S et al (2014) Soil C and N availability determine the priming effect: microbial N mining and stoichiometric decomposition theories. Glob Chang Biol 20(7):2356–2367. https://doi.org/10.1111/gcb.12475

Chen YP, Chen GS, Robinson D et al (2016) Large amounts of easily decomposable carbon stored in subtropical forest subsoil are associated with r-strategy-dominated soil microbes. Soil Biol Biochem 95:233–242. https://doi.org/10.1016/j.soilbio.2016.01.004

Chen YL, Du ZL, Weng Z et al (2023) Formation of soil organic carbon pool is regulated by the structure of dissolved organic matter and microbial carbon pump efficacy: a decadal study comparing different carbon management strategies. Glob Chang Biol 29(18):5445–5459. https://doi.org/10.1111/gcb.16865

Ding F, Van Zwieten L, Zhang WD et al (2018) A meta-analysis and critical evaluation of influencing factors on soil carbon priming following biochar amendment. J Soils Sediments 18(4):1507–1517. https://doi.org/10.1007/s11368-017-1899-6

Duan X, Li Z, Wang S et al (2025) Stability of iron-carbon complexes determines carbon sequestration efficiency in iron-rich soils. Soil Biol Biochem 203:109718. https://doi.org/10.1016/j.soilbio.2025.109718

Fierer N, Bradford MA, Jackson RB (2007) Toward an ecological classification of soil bacteria. Ecology 88(6):1354–1364. https://doi.org/10.1890/05-1839

Francioli D, Schulz E, Lentendu G et al (2016) Mineral vs. organic amendments: microbial community structure, activity and abundance of agriculturally relevant microbes are driven by long-term fertilization strategies. Front Microbiol 7:1446. https://doi.org/10.3389/fmicb.2016.01446

Fu YY, Xu YQ, Wang Q et al (2025) Deciphering the microbial players driving straw decomposition and accumulation in soil components of

particulate and mineral-associated organic matter. Soil Biol Biochem 209:109871. https://doi.org/10.1016/j.soilbio.2025.109871
Ghani A, Dexter M, Perrott KW (2003) Hot-water extractable carbon in soils: a sensitive measurement for determining impacts of fertilisation, grazing and cultivation. Soil Biol Biochem 35(9):1231–1243. https://doi.org/10.1016/S0038-0717(03)00186-X
Grant T, Sethuraman A, Escobar MA et al (2022) Chronic dry nitrogen inputs alter soil microbial community composition in Southern California semi-arid shrublands. Appl Soil Ecol 176:104496. https://doi.org/10.1016/j.apsoil.2022.104496
Hammarlund SP, Chacón JM, Harcombe WR (2019) A shared limiting resource leads to competitive exclusion in a cross-feeding system. Environ Microbiol 21(2):759–771. https://doi.org/10.1111/1462-2920.14493
Han LF, Sun K, Yang Y et al (2020) Biochar's stability and effect on the content, composition and turnover of soil organic carbon. Geoderma 364:114184. https://doi.org/10.1016/j.geoderma.2020.114184
Han CD, Chen L, Jia ZJ et al (2025) Organic amendments enhance rhizosphere carbon stabilization in macroaggregates of saline-sodic soils by regulating keystone microbial clusters. J Environ Manage 380:125086. https://doi.org/10.1016/j.jenvman.2025.125086
Helmke PA, Sparks DL (1996) Lithium, sodium, potassium, rubidium, and cesium. Methods of soil analysis, pp 551–574. https://doi.org/10.2136/sssabookser5.3.c19
Hu T, Wei JT, Du L et al (2023) The effect of biochar on nitrogen availability and bacterial community in farmland. Ann Microbiol 73(1):4. https://doi.org/10.1186/s13213-022-01708-1
Huang MZ, Hu TX, Wang JY et al (2024) Effects of biochar on soil carbon pool stability in the Dahurian larch (*Larix gmelinii*) forest are regulated by the dominant soil microbial ecological strategy. Sci Total Environ 951:175725. https://doi.org/10.1016/j.scitotenv.2024.175725
Jiang ZH, Liu YZ, Yang JP et al (2021) Rhizosphere priming regulates soil organic carbon and nitrogen mineralization: the significance of abiotic mechanisms. Geoderma 385:114877. https://doi.org/10.1016/j.geoderma.2020.114877
Kalu S, Seppanen A, Mganga KZ et al (2024) Biochar reduced the mineralization of native and added soil organic carbon: evidence of negative priming and enhanced microbial carbon use efficiency. Biochar. https://doi.org/10.1007/s42773-023-00294-y
Kuzyakov Y, Subbotina I, Chen HQ et al (2009) Black carbon decomposition and incorporation into soil microbial biomass estimated by $^{14}C$ labeling. Soil Biol Biochem 41(2):210–219. https://doi.org/10.1016/j.soilbio.2008.10.016
Lavallee JM, Soong JL, Cotrufo MF (2020) Conceptualizing soil organic matter into particulate and mineral-associated forms to address global change in the 21st century. Glob Chang Biol 26(1):261–273. https://doi.org/10.1111/gcb.14859
Lehmann J, Gaunt J, Rondon M (2006) Bio-char sequestration in terrestrial ecosystems—a review. Mitig Adapt Strateg Glob Change 11(2):403–427. https://doi.org/10.1007/s11027-005-9006-5
Lei KJ, Dai WX, Wang J et al (2024) Biochar and straw amendments over a decade divergently alter soil organic carbon accumulation pathways. Agronomy 14(9):2176. https://doi.org/10.3390/agronomy14092176
Leng LJ, Xiong Q, Yang LH et al (2021) An overview on engineering the surface area and porosity of biochar. Sci Total Environ 763:144204. https://doi.org/10.1016/j.scitotenv.2020.144204
Li LJ, Zhu-Barker X, Ye RZ et al (2018) Soil microbial biomass size and soil carbon influence the priming effect from carbon inputs depending on nitrogen availability. Soil Biol Biochem 119:41–49. https://doi.org/10.1016/j.soilbio.2018.01.003
Li F, Niu YX, Zhang JB et al (2023) The grape string theory is inspired by *Mortierella* and *Trichocladium* species that promote soil aggregation more than indigenous microorganisms. Geoderma 435:116524. https://doi.org/10.1016/j.geoderma.2023.116524
Liang C, Schimel JP, Jastrow JD (2017) The importance of anabolism in microbial control over soil carbon storage. Nat Microbiol 2:7105. https://doi.org/10.1038/nmicrobiol.2017.105
Liebich J, Vereecken H, Burauel P (2006) Microbial community changes during humification of $^{14}C$-labelled maize straw in heat-treated and native Orthic Luvisol. Eur J Soil Sci 57(4):446–455. https://doi.org/10.1111/j.1365-2389.2006.00815.x
Liu MH, Wei YQ, Lian L et al (2023) Macrofungi promote SOC decomposition and weaken sequestration by modulating soil microbial function in temperate steppe. Sci Tot Environ. https://doi.org/10.1016/j.scitotenv.2023.165556
Liu Q, Zhu ZK, Wei L et al (2025a) Bacterial necromass decomposition and priming effects in paddy soils depend on long-term fertilization. Soil Biol Biochem 211:109992. https://doi.org/10.1016/j.soilbio.2025.109992
Liu YD, Chen ZD, Li LH et al (2025b) Linking prokaryotic life-history strategies to soil organic carbon stability in semi-arid orchard with cover crops. CATENA 252:108833. https://doi.org/10.1016/j.catena.2025.108833
Lu YH, Watanabe A, Kimura M (2004) Contribution of plant photosynthates to dissolved organic carbon in a flooded rice soil. Biogeochemistry 71(1):1–15. https://doi.org/10.1007/s10533-004-3258-0
Luo L, Wang JX, Lv JT et al (2023) Carbon sequestration strategies in soil using biochar: advances, challenges, and opportunities. Environ Sci Technol 57(31):11357–11372. https://doi.org/10.1021/acs.est.3c02620
Lyu LH, Wang CQ, Fan KK et al (2025) Microbial life-history strategies mediate temperature effects on organic carbon pools in black soils. Soil Ecol Lett 7(3):250306. https://doi.org/10.1007/s42832-025-0306-2
Ma S, Zhu WZ, Wang WW et al (2023) Microbial assemblies with distinct trophic strategies drive changes in soil microbial carbon use efficiency along vegetation primary succession in a glacier retreat area of the southeastern Tibetan Plateau. Sci Total Environ 867:161587. https://doi.org/10.1016/j.scitotenv.2023.161587
Meng D, Zhang K, Liu ZP et al (2025) Refining amino sugar-based conversion factors for quantification of microbial necromass carbon in soils. Glob Change Biol 31(8):e70443. https://doi.org/10.1111/gcb.70443
Minasny B, Malone BP, McBratney AB et al (2017) Soil carbon 4 per mille. Geoderma 292:59–86. https://doi.org/10.1016/j.geoderma.2017.01.002
Mulvaney RL (1996) Nitrogen—inorganic forms. Methods of soil analysis, pp 1123–1184. https://doi.org/10.2136/sssabookser5.3.c38
Murphy J, Riley JP (1962) A modified single solution method for the determination of phosphate in natural waters. Anal Chim Acta 27:31–36. https://doi.org/10.1016/S0003-2670(00)88444-5
Nemergut DR, Cleveland CC, Wieder WR et al (2010) Plot-scale manipulations of organic matter inputs to soils correlate with shifts in microbial community composition in a lowland tropical rain forest. Soil Biol Biochem 42(12):2153–2160. https://doi.org/10.1016/j.soilbio.2010.08.011
Nordmeyer H, Richter J (1985) Incubation experiments on nitrogen mineralization in loess and sandy soils. Plant Soil 83(3):433–445. https://doi.org/10.1007/BF02184455
Okebalama CB, Marschner B (2023) Reapplication of biochar, sewage waste water, and NPK fertilizers affects soil fertility, aggregate stability, and carbon and nitrogen in dry-stable aggregates of semi-arid soil. Sci Total Environ 866:161203. https://doi.org/10.1016/j.scitotenv.2022.161203
Phung NT, Lee J, Kang KH et al (2004) Analysis of microbial diversity in oligotrophic microbial fuel cells using 16S rDNA sequences. FEMS Microbiol Lett 233(1):77–82. https://doi.org/10.1016/j.femsle.2004.01.041
Salas E, Gorfer M, Bandian D et al (2023) A rapid and sensitive assay to quantify amino sugars, neutral sugars and uronic acid necromass biomarkers using pre-column derivatization, ultra-high-performance liquid chromatography and high-resolution mass spectrometry. Soil Biol Biochem 177:108927. https://doi.org/10.1016/j.soilbio.2022.108927
Shang WH, Razavi BS, Yao SH et al (2023) Contrasting mechanisms of nutrient mobilization in rhizosphere hotspots driven by straw and biochar amendment. Soil Biol Biochem 187:109212. https://doi.org/10.1016/j.soilbio.2023.109212
Singh N, Abiven S, Maestrini B et al (2014) Transformation and stabilization of pyrogenic organic matter in a temperate forest field experiment. Glob Change Biol 20(5):1629–1642. https://doi.org/10.1111/gcb.12459
Smith JL, Collins HP, Bailey VL (2010) The effect of young biochar on soil respiration. Soil Biol Biochem 42(12):2345–2347. https://doi.org/10.1016/j.soilbio.2010.09.013
Song HM, Chang ZX, Hu X et al (2024) Combined application of chemical and organic fertilizers promoted soil carbon sequestration and bacterial community diversity in dryland wheat fields. Land 13(8):1296. https://doi.org/10.3390/land13081296
Souza TP, Marques SC, da Silveira e Santos DM et al (2014) Analysis of thermophilic fungal populations during phase II of composting for the cultivation of *Agaricus subrufescens*. World J Microbiol Biotechnol 30(9):2419–2425. https://doi.org/10.1007/s11274-014-1667-3
Tivet F, de Moraes Sa JC, Lal R et al (2013) Soil organic carbon fraction losses upon continuous plow-based tillage and its restoration by diverse

biomass-C inputs under no-till in sub-tropical and tropical regions of Brazil. Geoderma 209:214–225. https://doi.org/10.1016/j.geoderma.2013.06.008

Vance ED, Brookes PC, Jenkinson DS (1987) An extraction method for measuring soil microbial biomass C. Soil Biol Biochem 19(6):703–707. https://doi.org/10.1016/0038-0717(87)90052-6

Wang QY, Yuan J, Yang X et al (2022) Responses of soil respiration and C sequestration efficiency to biochar amendment in maize field of Northeast China. Soil Tillage Res 223:105442. https://doi.org/10.1016/j.still.2022.105442

Wang H, Guo YF, Fang HJ et al (2025a) Divergent effects of straw and straw-derived biochar on soil N transformation and $N_2O$ emissions: a global meta-analysis. J Environ Manage 395:127784. https://doi.org/10.1016/j.jenvman.2025.127784

Wang H, Ye WH, He W et al (2025b) Phosphorus addition increases soil organic matter priming in a coastal saline soil. Soil Biol Biochem 208:109862. https://doi.org/10.1016/j.soilbio.2025.109862

Wang R, Hou JH, Chen LT et al (2025c) Priming effects of vermiculite modified rice straw biochar on soil organic carbon: a new perspective of soil bacteria. Biochar 7(1):54. https://doi.org/10.1007/s42773-025-00440-8

Wang JG, Wei K, Jing YL et al (2026) Soil microbivorous nematodes contribute to the formation of microbial necromass carbon under full straw return. Agric Ecosyst Environ 396:109975. https://doi.org/10.1016/j.agee.2025.109975

Weisburg WG, Bs F, Pelletier DA et al (1991) 16S ribosomal DNA amplification for phylogenetic study. J Bacteriol 173(2):697–703. https://doi.org/10.1128/jb.173.2.697-703.1991

Weng Z, Van Zwieten L, Singh BP et al (2017) Biochar built soil carbon over a decade by stabilizing rhizodeposits. Nat Clim Chang 7(5):371–376. https://doi.org/10.1038/nclimate3276

Wu XJ, Liu PF, Wegner CE et al (2021) Deciphering microbial mechanisms underlying soil organic carbon storage in a wheat-maize rotation system. Sci Total Environ 788:147798. https://doi.org/10.1016/j.scitotenv.2021.147798

Wu Q, Zhang YX, Zhao L et al (2025) Strategies for efficient degradation of lignocellulose from straw: synergistic effects of acid-base pretreatment and functional microbial agents in composting. Chem Eng J 508:161048. https://doi.org/10.1016/j.cej.2025.161048

Xie NH, Fan YC, Duan N et al (2025) Interactive effects of straw and biochar amendments on soil organic carbon stabilization and bacterial community dynamics. Biol Fertil Soils 61(8):1423–1437. https://doi.org/10.1007/s00374-025-01947-9

Xu RS, Zhang YH, Li Y et al (2024) Linking bacterial life strategies with the distribution pattern of antibiotic resistance genes in soil aggregates after straw addition. J Hazard Mater 471:134355. https://doi.org/10.1016/j.jhazmat.2024.134355

Yang CD, Liu JJ, Ying HC et al (2022) Soil pore structure changes induced by biochar affect microbial diversity and community structure in an Ultisol. Soil Tillage Res 224:105505. https://doi.org/10.1016/j.still.2022.105505

Yang CD, Chang YX, Liu J et al (2025a) Differences in the physical protection mechanisms of soil organic carbon with $^{13}C$-labeled straw and biochar. Biochar 7(1):32. https://doi.org/10.1007/s42773-025-00430-w

Yang H, Yang YH, Zhu HQ et al (2025b) Short-term phosphorus fertilization alters soil fungal community in long-term phosphorus-deprived yellow soil paddy fields. Agriculture 15(3):280. https://doi.org/10.3390/agriculture15030280

Yang ZM, Charoenkal K, Wang ZC et al (2025c) Ammonium recovery from wastewater by biochar with different N/O-doped groups and hierarchical pores: synergistic enhancement mechanisms for strong negative electrostatic potential and micropore filling. J Environ Manage 386:125776. https://doi.org/10.1016/j.jenvman.2025.125776

Yang L, Luo JQ, Gu CM et al (2026) Preceding intercropped leguminous green manure shifts microbial life strategies to regulate soil organic carbon in low-nitrogen input maize-rapeseed rotations. Soil Tillage Res 256:106841. https://doi.org/10.1016/j.still.2025.106841

Yao MJ, Rui JP, Niu HS et al (2017) The differentiation of soil bacterial communities along a precipitation and temperature gradient in the eastern Inner Mongolia steppe. CATENA 152:47–56. https://doi.org/10.1016/j.catena.2017.01.007

Yu Z, Chen L, Pan S et al (2018) Feedstock determines biochar-induced soil priming effects by stimulating the activity of specific microorganisms. Eur J Soil Sci 69(3):521–534. https://doi.org/10.1111/ejss.12542

Zeng J, Xing LH, Li Y et al (2025) Divergent mechanisms of rhizosphere and non-rhizosphere soil organic carbon sequestration under precipitation variability: evidence from microbial life-history strategies. Appl Soil Ecol 213:106302. https://doi.org/10.1016/j.apsoil.2025.106302

Zhang XD, Amelung W (1996) Gas chromatographic determination of muramic acid, glucosamine, mannosamine, and galactosamine in soils. Soil Biol Biochem 28(9):1201–1206. https://doi.org/10.1016/0038-0717(96)00117-4

Zhang H, Liu YJ, Nie XQ et al (2018) The cyanobacterial ornithine–ammonia cycle involves an arginine dihydrolase. Nat Chem Biol 14(6):575–581. https://doi.org/10.1038/s41589-018-0038-z

Zhang YY, Wang T, Yan C et al (2024a) Microbial life-history strategies and particulate organic carbon mediate formation of microbial necromass carbon and stabilization in response to biochar addition. Sci Total Environ 950:175041. https://doi.org/10.1016/j.scitotenv.2024.175041

Zhang ZJ, Zhao YN, Li ZG et al (2024b) Vegetation drives soil microbial metabolic limitation through modifications of soil properties and microbial biomass during desert grassland-shrubland state anthropogenic transition. Appl Soil Ecol 202:105609. https://doi.org/10.1016/j.apsoil.2024.105609

Zhao SX, Ta N, Wang XD (2017) Effect of temperature on the structural and physicochemical properties of biochar with apple tree branches as feedstock material. Energies 10(9):1293. https://doi.org/10.3390/en10091293

Zhou GP, Li GL, Liang H et al (2025a) Green manure coupled with straw returning increases soil organic carbon via decreased priming effect and enhanced microbial carbon pump. Glob Change Biol 31(5):e70232. https://doi.org/10.1111/gcb.70232

Zhou RR, Chen WJ, Gunina A et al (2025b) Carbon sequestration through straw amendment: multi-pool dynamics within soil organic carbon. Geoderma 461:117471. https://doi.org/10.1016/j.geoderma.2025.117471